Analyses of Near-Field and Near-Regional Signals from the Black Thunder Mine

Terrance G. Barker
Keith L. McLaughlin

Maxwell Technologies, Inc.
8888 Balboa Avenue
San Diego, CA 92123-1506

February 1998

Final Report

10 August 95 - 9 August 97

Approved for public release; distribution unlimited

DEPARTMENT OF ENERGY
Office of Nonproliferation and National Security
WASHINGTON, DC 20585

AIR FORCE RESEARCH LABORATORY
Space Vehicles Directorate
29 Randolph Rd
Hanscom AFB, MA 01731-3010

DTIC QUALITY INSPECTED 4

REPORT DOCUMENTATION PAGE

1. AGENCY USE ONLY (Leave blank)	2. REPORT DATE	3. REPORT TYPE AND DATES COVERED
	February 1998	Final (10 August 1995 - 9 August 1997)

4. TITLE AND SUBTITLE

Analysis of Near-Field and Near-Regional Signals from the Black Thunder Mine

5. FUNDING NUMBERS

Contract No. F19628-95-C-0112

PE 6912OH
PR DENN TA GM WU AV

6. AUTHOR(S)

Terrance G. Barker, Keith L. McLaughlin

7. PERFORMING ORGANIZATION NAME(S) AND ADDRESS(ES)

Maxwell Technologies, Inc.
Federal Division
8888 Balboa Avenue
San Diego, CA 92123-1506

8. PERFORMING ORGANIZATION REPORT NUMBER

MFD-DTR-98-15992

9. SPONSORING/MONITORING AGENCY NAME(S) AND ADDRESS(ES)

Air Force Research Laboratory
29 Randolph Road
Hanscom AFB, MA 01731-3010
Contract Manager: Katharine Kadinsky-Cade/VSBS

10. SPONSORING/MONITORING AGENCY REPORT NUMBER

AFRL-VS-HA-TR-98-0033

11. SUPPLEMENTARY NOTES

This research was sponsored by the Department of Energy, Office of Non-Proliferation and National Security, Washington, DC 20585

12a. DISTRIBUTION/AVAILABILITY STATEMENT

Approved for public release; distribution unlimited

12b. DISTRIBUTION CODE

13. ABSTRACT (Maximum 200 words)

In this report we present analyses of seismic data recorded at the Black Thunder coal strip mine in the Powder River Basin of Wyoming. The data (collected by Stump et al., 1996) are a set of recordings at distances of a few kilometers from mining activity at that mine. Our objective was to determine whether these near-field data revealed features of quarry blasting that were unique to that source type. In our previous annual report on this research contract (Barker et al., 1997) and in Bonner et al. (1997), we described analyses of near-regional surface waves from a quarry in Texas. Their analyses used numerical simulations and predictions of the kinematic model in Barker et al. (1993) to interpret the dependence of amplitudes on azimuth in terms of quarry geometry and mass movement. Our objective in the current study was to apply these results to the recorded explosions at the Black Thunder mine. We find the following: Continues . . .

14. SUBJECT TERMS

Seismic   Test Ban Treaty   Source Identification   Quarry Blasts

15. NUMBER OF PAGES

52

16. PRICE CODE

17. SECURITY CLASSIFICATION OF REPORT	18. SECURITY CLASSIFICATION OF THIS PAGE	19. SECURITY CLASSIFICATION OF ABSTRACT	20. LIMITATION OF ABSTRACT
Unclassified	Unclassified	Unclassified	SAR

CLASSIFIED BY:

DECLASSIFIED ON:

13. ABSTRACT (Continued)

1. Ripple firing effectively low pass filters the signals, in agreement with previous studies. Since for the near-field signals at Black Thunder, the observed high frequency components of the signals are associated with P waves and the lower frequency signals are associated with surface waves (dominated by shear motion), ripple firing has the indirect effect of increasing the S/P ratio in the seismograms.

2. We observe no consistent differences between motions from cast blasts and coal shots, nor between cast shots in which the throw or strike of the bench is different. This is due to the dominance of ground motion due to explosions relative to that caused by mass movement, which is in turn is due to relative source coupling or propagation. Since differences in mass movement are the primary differences in the source mechanisms between coal and cast blasts, the dominance of the explosion component obscures the source mechanism.

3. Vertical and tangential near field ground motions (corrected for site response) from cast blasts are strongly enhanced normal to the bench in the direction of unmined land. We have no azimuthal coverage of a coal shot.

In addition to studies of near-field data, we analyzed near-regional data presented by Hedlin *et al.*, (1996). In the summer of 1996, IGPP/UCSD deployed five seismometers at ranges between 100 and 200 km from the Black Thunder mine, which augment the permanent regional stations RSSD and PDAR. After correcting for propagation, we have examined the data for dependence on azimuth and source location. The data are from shots in two pits that are perpendicular to each other and include a shot in which a fraction of the charges detonated simultaneously. The corrected ground motions show no azimuthal dependence on shot orientation.

TABLE OF CONTENTS

FIGURES

TABLES

1.0   Introduction

In this report we present analyses of seismic data recorded at the Black Thunder coal strip mine in the Powder River Basin of Wyoming. The data (collected by Stump *et al.*, 1996) are a set of recordings at distances of a few kilometers from mining activity at that mine. Our objective was to determine whether these near-field data revealed features of quarry blasting that were unique to that source type. All the mining activity involved explosions, of course, but they were designed to suit different purposes whose differences could potentially be used to isolate aspects of quarry blast sources. In this series were standard quarry cast blasts that were designed to fracture and cast material from a bench onto the mine floor. Another source type was the coal shot that was detonated in the mine floor. The purpose of coal shots is to fracture ("bulk") the coal prior to excavation and involves very little net movement of the fractured material. To reduce ground roll to neighboring areas and enhance fracturing, both of these shot types are ripple-fired. The data also include recordings of a coal shot which was not ripple-fired (all charges were detonated simultaneously), done by the mine operators at the request of the experimenters for the purpose of studying the effects of ripple-firing on seismic signals.

Each shot type, then, had an explosive component, with the ripple-fired shots having an extended source duration. The coal shots heaved the ground vertically (as can be seen in video recordings), so there should be a seismic force associated with the ballistic (spall) motion of the heaved material similar to that observed in nuclear explosions. Indeed, we approached the analysis assuming the coal shots could be modeled along the lines of an underburied nuclear explosion with an explosive component and spall component, as proposed by several authors (Day and McLaughlin, 1991, Barker *et al.*, 1993a, Taylor and Randall, 1989). Cast blasts involve mass movement that has both vertical and horizontal net displacement. Barker *et al.* (1993b), proposed a kinematic model of cast blasts that included vertical and horizontal net displacement, and this model provided the conceptual framework for studying the cast blast signals.

In addition to the three source types mentioned above, other source variables included bench location and throw direction. In our annual report on the first year of this research contract (Barker *et al.*, 1997) and in Bonner *et al.* (1996), we described analyses of near-regional surface waves from a quarry in Texas. Their analyses used numerical simulations and predictions of the kinematic model in Barker *et al.* (1993b) to interpret the dependence of amplitudes on azimuth in terms of quarry geometry and mass movement. Our objective in the current study was to apply these results to the recorded explosions at the Black Thunder mine.

In addition to studies of near-field data, we analyzed near-regional data presented by Hedlin *et al.*, (1996). In the summer of 1996, IGPP/UCSD deployed five seismometers at ranges between 100 and 200 km from the Black Thunder mine, which augment the permanent regional stations RSSD and PDAR. After correcting for propagation, we have examined the data for dependence on azimuth and source location. The data are from shots in two pits that are perpendicular to each other and include a shot

1

in which a fraction of the charges detonated simultaneously. The corrected ground motions show no azimuthal dependence on shot orientation.

Surficial sedimentary layers made analysis of signals at the Black Thunder mine difficult. Inspection of the seismograms shows that the ground motions are strongly influenced by local earth structure. Signals at 11 km have duration exceeding 25 seconds, which greatly exceeds the duration of ripple firing and ballistic motion of the material. Since structure is so important, and we have no independent measurements of seismic velocity, we have inferred a velocity model from the blast data. We began with kinematic models of the quarry blasts based on blast design. We computed synthetic seismograms from plane-layered earth models which were modified to match essential features of the observed seismograms. Having no absolute timing information, the features were the shape and duration of the signals. Comparison of the derived earth structure with recent borehole measurements give us confidence in the results.

A difficulty encountered in the interpretation of these data is a lack of statistical confidence. That is, rarely were shots of the same type in the same pit recorded on seismometers at the same place. Thus, we could not reliably observe the effects of varying one parameter while holding others fixed. The data we have are good quality, but logistical constraints on the experimenters limited the breadth of the data set (B. Stump and C. Pearson, private communication). Nevertheless, we proceeded with the analysis and make the following conclusions.

1. Ripple firing effectively low pass filters the signals, in agreement with previous studies. Since for the near-field signals at Black Thunder, the observed high frequency components of the signals are associated with P waves and the lower frequency signals are associated with surface waves (dominated by shear motion), ripple firing has the indirect effect of increasing the S/P ratio in the seismograms.

2. We observe no consistent differences between motions from cast blasts and ripple-fired coal shots. In our previous numerical studies under this contract (Barker *et al.*, 1997) and in field studies (Bonner *et al.* 1996), azimuthal variations due to throw or strike of the bench were predicted and observed. We observe no differences between cast shots at the Black Thunder mine in which the throw or strike of the bench is different. We examined differences in seismogram character, S/P ratio and spectral slope. The lack of differences is due to the dominance of ground motion caused by explosions relative to that caused by mass movement, which is in turn is due to relative source coupling or propagation. Since differences in mass movement are the primary differences in the source mechanisms between coal and cast blasts, the dominance of the explosion component obscures the source mechanism.

3. Vertical and tangential near field ground motions (corrected for site response) from cast blasts are strongly enhanced normal to the bench in the direction of unmined land. We have no azimuthal coverage of a coal shot.

4. In contrast to the results of our previous studies in Texas (Barker *et al.*, 1997, Bonner *et al.* 1996), near-regional ground motions (corrected for path) show no azimuthal dependence on shot orientation, presumably for the same reasons azimuthal variations are not observed in the near field data.

2.0 Experimental Setup, Mine Description and Description of Near-Field Data

Data from several shots in the South, West and Northeast Pits, described in Stump *et al.* (1996), were made available to us by Dr. Craig Pearson at LANL. The field layout is shown in Figure 1. Shot descriptions are given in Table 1. Descriptions of the sensors and experimental procedures can be found in Stump *et al.* (1996).

There are two main shot types in this data set: <u>cast shots</u> which are designed to move material from a bench to the floor of the mine and <u>coal shots</u> which fracture the material in the floor of the mine. Coal shots are meant to move material vertically only. Both these shots are ripple-fired. A third shot type is a simultaneous coal shot where all charges in this blast were detonated simultaneously. Mining operations have proceeded from north to south, and the land is reclaimed after coal is removed.
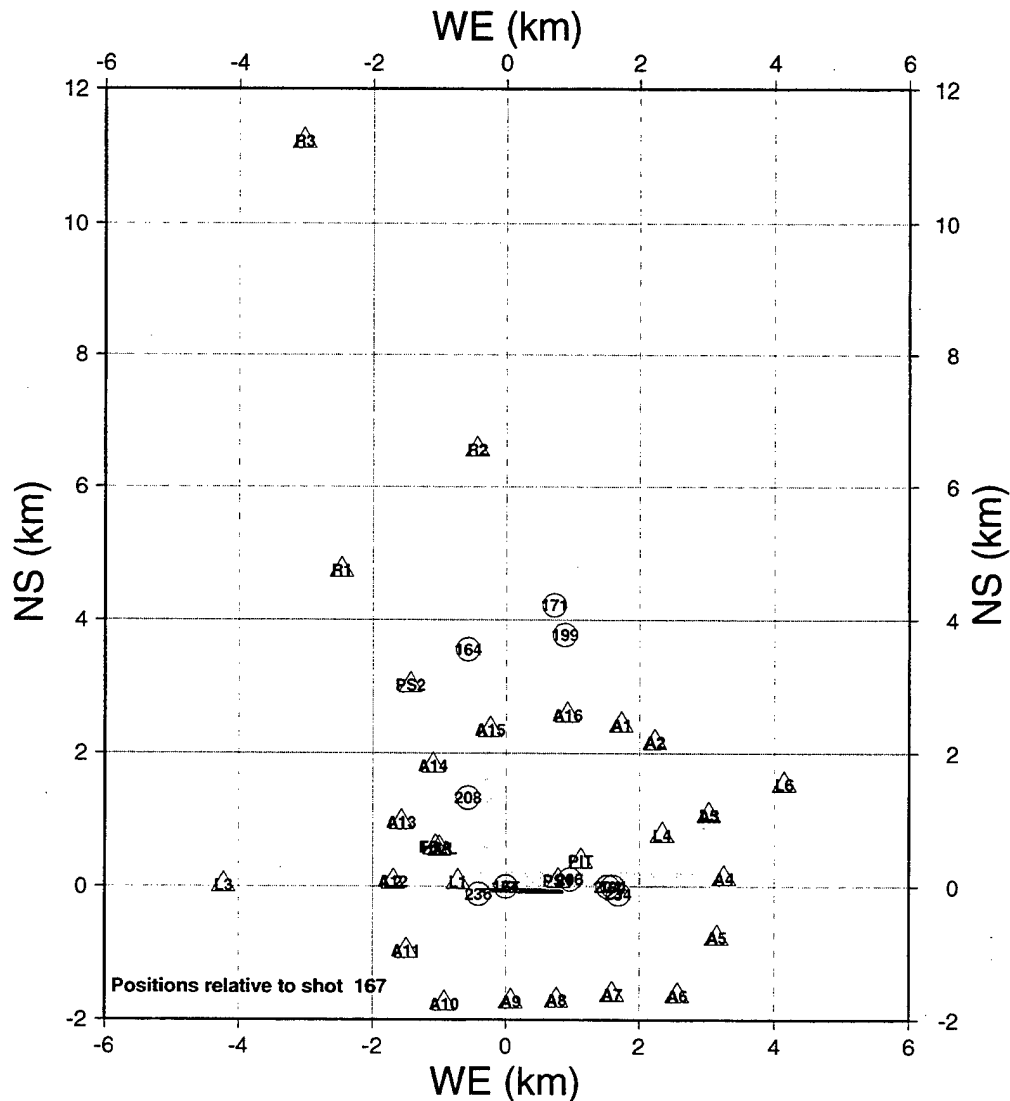
Figure 1. Locations of shots (circles) and recorders (triangles) relative to shot 167. The West and South Pits are shown as stippled areas.

Table 1. Shot descriptions.

shot	TYPE	PIT	W (kT)
s167	cast	S	4.41
s174	cast	S	1
s236	Simultaneous coal	S	0.002
s171	coal	NE	0.05
s184	coal	S	0.07
s193	cast	S	0.16
s199	cast	NE	1.66
s204	coal	S	0.16
s206	cast	S	1.55
s208	coal	W	0.08

A matrix showing source-receiver combinations for which we were provided data is displayed in Table 2. To isolate the effects of source and propagation on radiation patterns, distance dependence and seismogram attributes such as duration, and P to S ratio, we would ideally have data at multiple azimuths and distances from different shot types and different shot locations (pits). Of course, some degree of repeatability is useful. Although we were provided with a large amount of high quality data, they generally did not fulfill these requirements. The "A" stations (see Figure 1) form a ring around the center of the south pit at a radius of about 2 km. However, they were deployed for only two cast blasts in the South Pit and for no coal shots. The "R" stations, which form a line along a roughly NNW azimuth, recorded shots of each type and were useful for studying the effects of source type (although the shots were in different pits), but the line is obviously along only one azimuth.

By way of introduction to the nature of the near-field ground motions in this data set, we show in Figure 2 the vertical ground motions from shot 167 (see Table 1) recorded at station R3 at a distance of about 13 km and heading NNW from the shot. This figure illustrates several features of the signals typical of this data set. Perhaps the most striking feature is the duration of the signals, which is 25 to 30 seconds. Since the duration of the detonations and subsequent mass movement are only a few seconds, the length of the wave trains are due to propagation. As is discussed in Section 5, the long wave trains are surface waves with a dominant frequency of 1 Hz travelling in low velocity surficial layers. The higher frequency, earlier arriving signals are shallow P waves. In general, the surface waves are several times larger than the P waves.

Table 2. Source-receiver matrix (available data indicated by x's).

Shot receiver	s167	s174	s236	s171	s184	s193	s199	s204	s206	s208
A1	x	x								
A2	x	x								
A3	x	x								
A4	x	x								
A5	x	x		x						
A6	x	x	x	x	x	x	x	x	x	x
A7	x	x		x						
A8	x	x		x						
A9	x	x		x						
A10	x	x								
A11	x	x		x						
A12	x	x	x			x				
A13	x	x	x	x	x	x	x	x	x	x
A14	x	x								
A15	x	x								
A16	x			x						
R1	x	x	x	x	x		x	x	x	x
R2	x	x	x	x	x	x	x	x	x	x
R3	x	x	x	x	x	x	x	x	x	x
R4						x	x	x	x	x
R5						x	x			
R6						x	x			
R7						x	x			
R8						x	x			
R9						x	x			
R10						x	x			
R11							x			
R12				x		x				
L1										
L2	x	x	x	x		x				
L3				x						
L4										
L5	x	x		x						
L6			x							
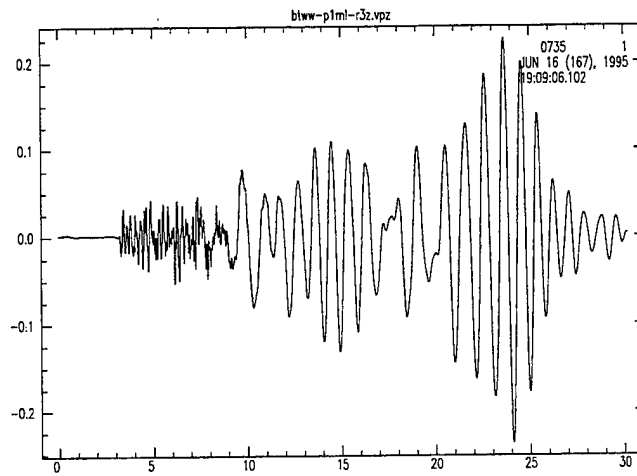
Figure 2. Vertical seismogram from shot 167 (see Table 1) recorded at station R3.

3.0   Effects of Ripple Firing

The recordings for which we have the most complete coverage are three South Pit shots. The shots are two large ripple-fired cast shots, and the simultaneous coal shot (see Table 1). Figure 1 shows the location of the pit (stippled area) at the time of these shots. Mining operations have proceeded from north to south, and the land is reclaimed after coal is removed. Thus, the highwall is on the south side of the pit. The cast blasts originated at nearly the same location, with shot 167 (4.7 million lbs.) propagating to the right, ending at the edge of the pit, and shot 174 (2.3 million lbs.) propagating to the left. The material was thrown to the NE by shot 167 and to the NW by shot 174. The coal shot (day 236) is west of shot 167 near the western end of the South Pit.

The duration of the signals is affected by the firing patterns, albeit to a lesser degree than by propagation. We can examine the effects of source duration by convolving the firing sequences of the cast blasts with the simultaneous coal shot. That is, we treat the simultaneous coal shot as a propagation Green's function. The shot durations (Figure 3) are several seconds. Figure 4 shows the results of the convolutions. From Figure 4, we see that the effects of the firing pattern time history are to (1) increase the duration of the signals and (2) increase the ratio of peak surface wave amplitude to P wave. The surface-to-P-wave-ratios of the convolutions and of the simultaneous coal shot are smaller than those of the cast blasts. We note that a fairly good fit to the cast blast records was achieved using the coal shot as a Green's function, which indicates that large mass movements affect the signals less than the explosive component.
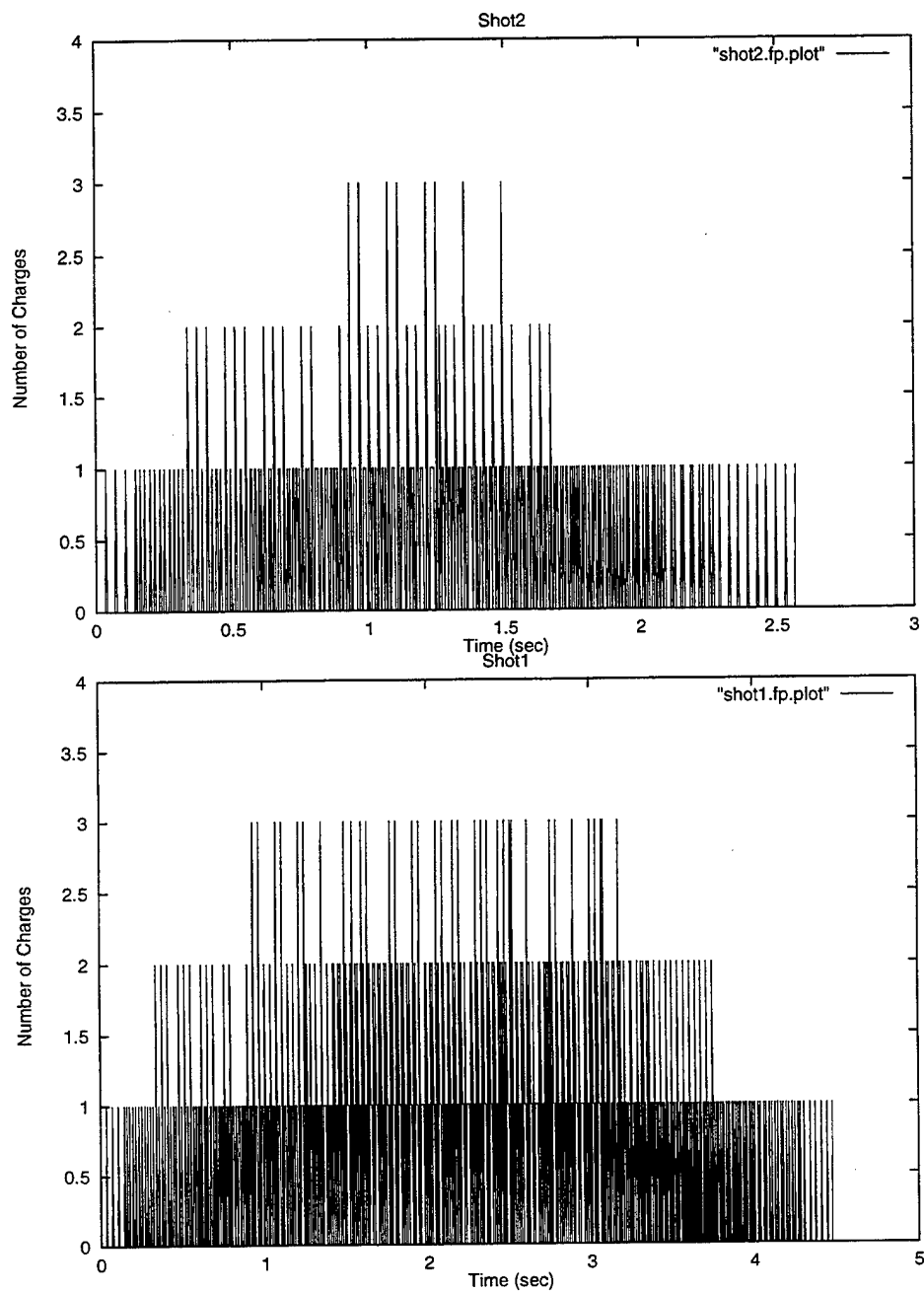
Figure 3. Firing pattern time series for shots 167 (above) and 174 (below).

stn r3, z component, shots 1 and 2, highpass npoles 8 corner 1.

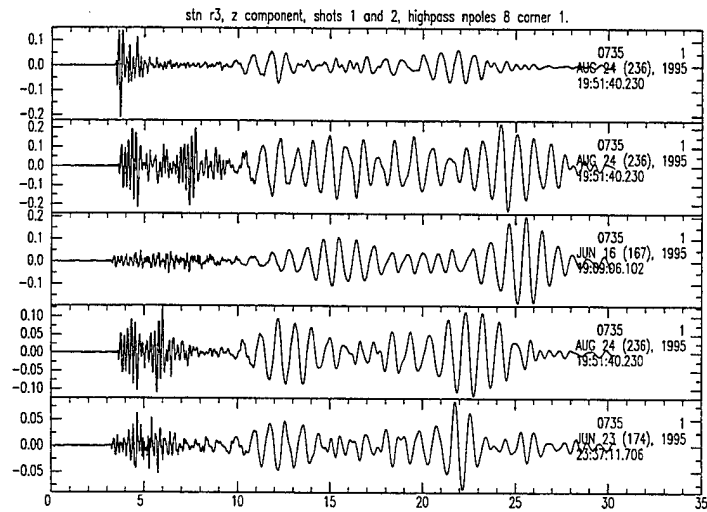Figure 4. Time series from top to bottom are (1) the simultaneous coal shot 236, (2) coal shot 236 convolved with the firing pattern for cast blast 167, (3) cast blast 167, (4) the coal shot convolved with the firing pattern for cast blast 174, and (5) cast blast 174.

10

4.0   Radiation Patterns

We now consider the radiation patterns from these shots using recordings at the "A" stations (Figure 1), which encircle the shots. The response at the "A" stations is strongly influenced by the local site conditions, in particular, whether the site was on unmined or reclaimed land (Barker *et al.*, 1996). In our previous work, we used the coda of signals from the shots themselves to estimate site responses. This gave site corrections and amplitudes corrected for site response which were substantially different for the two cast blasts, indicating that the responses were not good estimates. We show in the following the results of using the coda of signals from distant shots in the Powder River Basin to estimate site response. The site responses using the powder River Basin shots gave results that were quite consistent from shot to shot. Figures 5 and 6 show radiation patterns of peak amplitudes of the large cast blasts, corrected for response computed from the Powder River Basin coda. Peak amplitudes are associated with surface waves with frequencies near one Hz (e.g., the energy arriving between 10 and 30 seconds in Figure 2).

Mining operations at Black Thunder have progressed in a generally north to south direction. After mining, the land is filled, or reclaimed. Stations A1 through A5 and A15 are on reclaimed land and stations A6 through A14 are on unmined land. Uncorrected peak motions are larger on unmined land and smaller on reclaimed land (Barker *et al.*, 1996), while the converse is true for corrected amplitudes. In light of the complexities of the shots and the mine setting, the patterns are quite consistent. Both components of motion show strong amplification to the south. Amplification of motion behind the bench is consistent with previous studies. The radiation patterns appear to be insensitive to the throw of materials by the explosions.

Figure 5. Polar radiation patterns of peak vertical amplitudes of the large cast blasts (167 on left, 174 on the right), corrected for response computed from the Powder River Basin coda. Bold station names are on reclaimed land and faded station names are on unmined land.
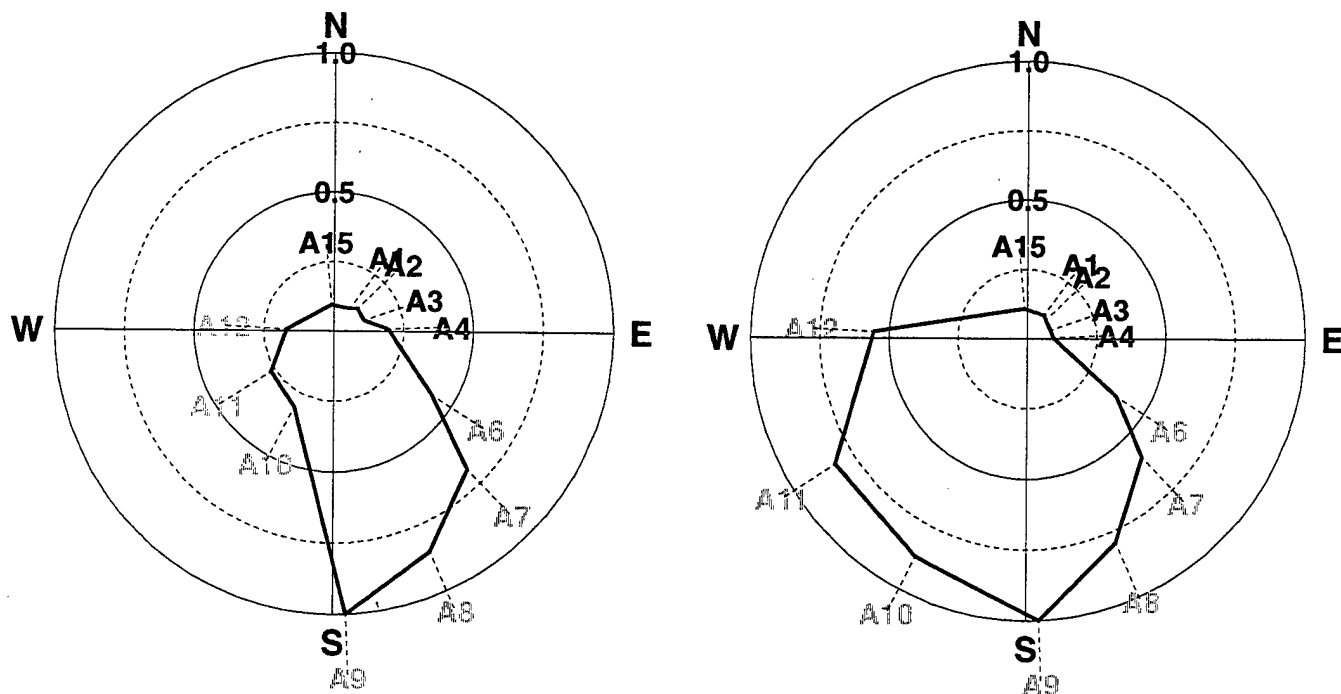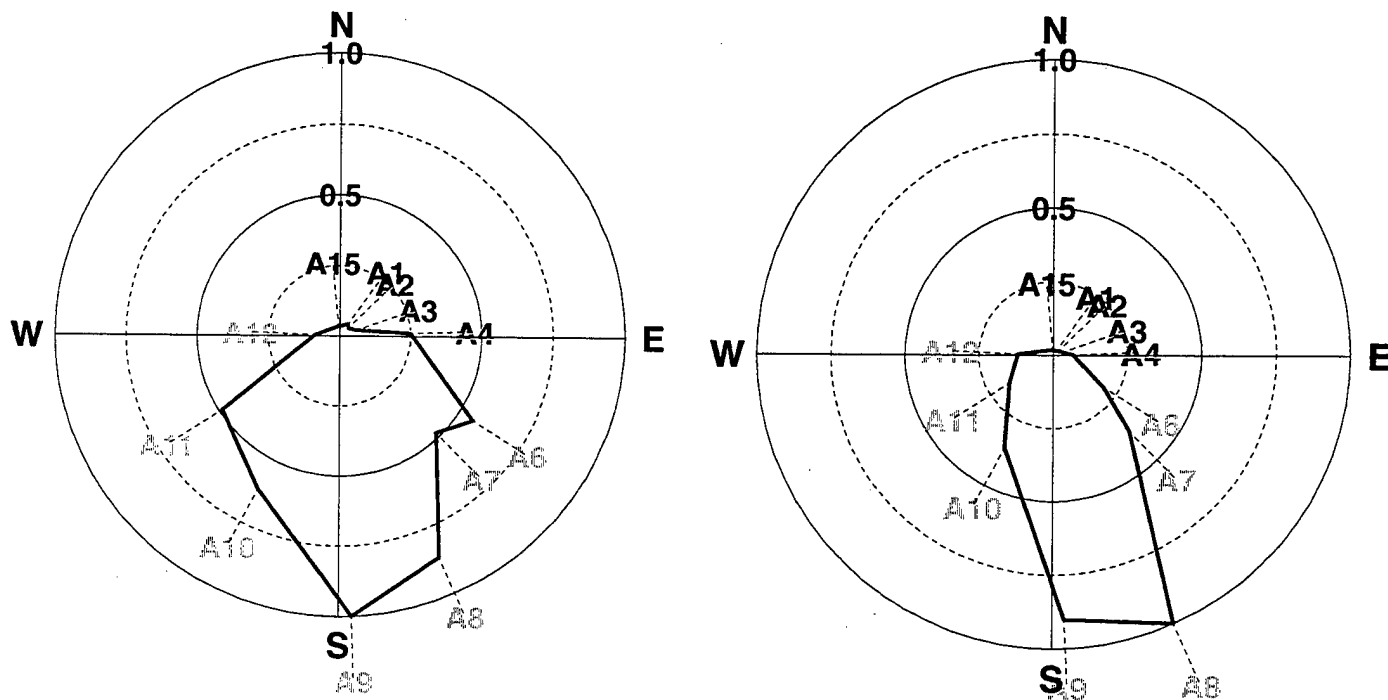

Figure 6. Polar radiation patterns of peak tangential amplitudes of the large cast blasts (167 on left, 174 on the right), corrected for response computed from the Powder River Basin coda. Bold station names are on reclaimed land and faded station names are on unmined land.

The equivalent force model predicts amplification of SH motion normal to the throw of spalled material and amplification of SV motion parallel to the throw. The explosive component and the vertical movement of material would contribute isotropic motions only in the vertical direction. Recall that the direction of throw for shots 167 and 174 differ by 90^0. The observed radiation patterns do not reflect this difference.

Bonner and Goforth (1995) noticed that the character of seismograms from a central Texas quarry were correlated with the orientation of the active quarry face as the quarry operations migrated within the quarry. In a subsequent study with good azimuthal coverage of a few blasts at the Chemline quarry, Bonner et al. (1996) inferred Rg radiation patterns from phase matched filtered Rg. They found Rg was enhanced behind the bench and attenuated for paths crossing the quarry floor. Delitsyne et al. (1996) studied intermediate period Love waves from quarry blasts in Siberia. They found that the polarity of Love waves on opposing quarry faces were reversed and that blasts in the floor of the quarry produced small Love waves compared to Rg. They concluded that the Love wave polarity reversals and amplitude dependence were consistent with a spall mechanism for the generation of Love waves from the quarry faces and opening of a vertical tension crack for blasts in the quarry floor as suggested by the master crack model of Konya and Walter (1990).

Two possible mechanisms for such non-isotropic radiation are 1) the lateral throw of spalled material, and 2) the presence of the topographic bench in the quarry (Barker et al., 1993a,b; and McLaughlin et al., 1994). The spall of material can be modeled by vertical and horizontal forces applied to the free surface with time functions proportional to the derivative of the momentum of the spalled material.

Barker et al. (1996) modeled the Chemline data (Bonner et al., 1996) using finite difference computations to account for the quarry geometry and synthetic seismogram calculations using the equivalent force model in Barker et al., (1993a). The radiation patterns of Love waves in the numerical simulations exhibit minima at azimuths perpendicular to the face of the quarry and maxima parallel to the quarry faces. Rayleigh waves (Rg) are enhanced behind the quarry face. The Love wave (SH or transverse) radiation patterns are similar to the observed radiation patterns at the Chemline quarry. However, the observed radiation patterns in Rg cannot be produced by the topographic bench alone. The observed enhancement of Rg behind the bench is much larger than can be explained by the topographic effects. This is also the case for the Black Thunder data.

5.0 Differences Due to Source Type

In the following, we explore the differences between signals from the two source types: coal shot and cast blast. We begin with qualitative observations in the time and frequency domain. We show a seismogram and spectrogram in Figures 7 through 9 for cast blasts 167 and 174 and coal shot 193, recorded at station R3. Both shots were in the south pit. We will focus on station R3 in this section of the report, but the conclusions reached here apply to other stations. Each of the seismograms can be characterized by a small, early arriving, broad band P wave train in the first 5 seconds of the record, followed by a larger, narrow band (1 to 2 Hz) surface wave whose duration is about 20 seconds. The largest motions occur at different times for each shot. There appear to be spectral nulls on the coal shot spectrogram between 10 and 12 seconds at about 5 Hz intervals. Generally speaking, however, the differences between the signals from the two shot types are as great as the differences between the signals from the two cast blasts. This comment applies to the radial and tangential components as well.
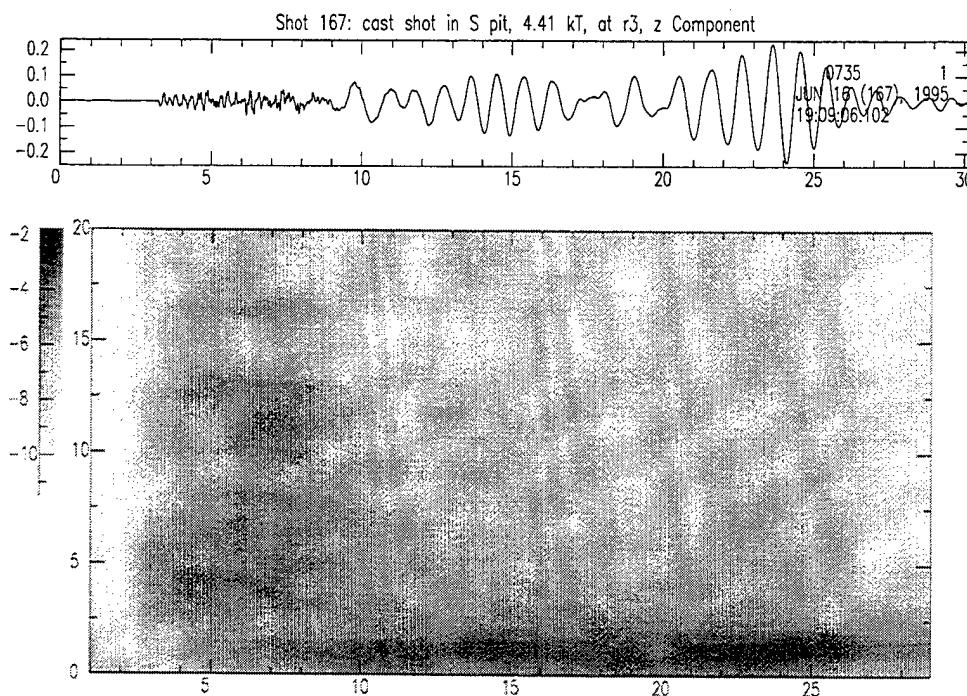
Figure 7. Seismogram and spectrogram (vertical component) for cast blast 167 in the south pit, recorded at station R3. Amplitude scale of the spectrogram (on the left) is in log units.

14
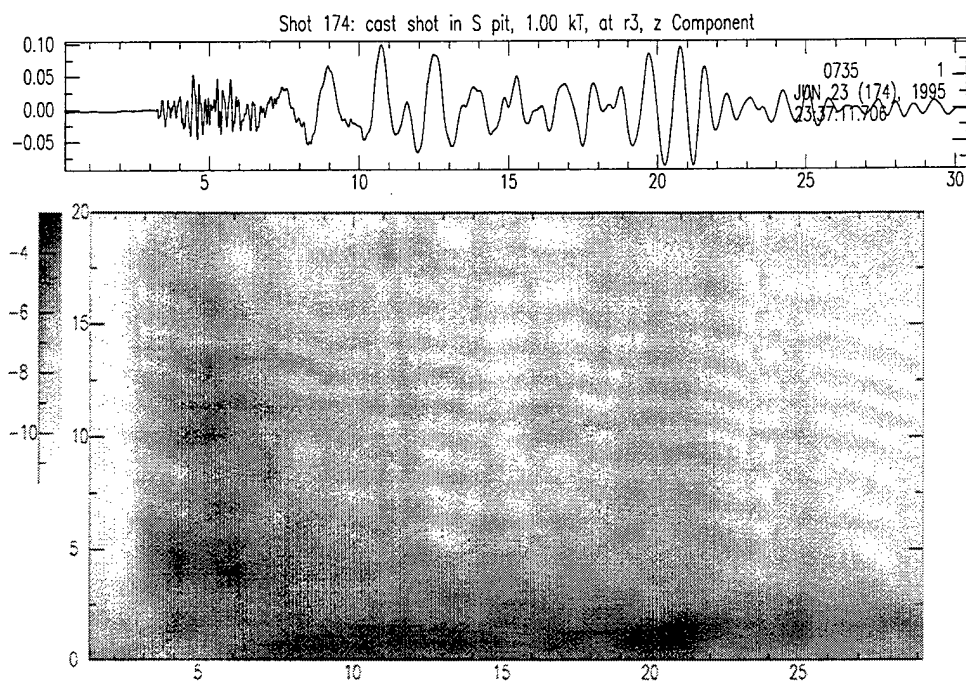
Figure 8. Seismogram and spectrogram (vertical component) for cast blast 174 in the south pit, recorded at station R3.
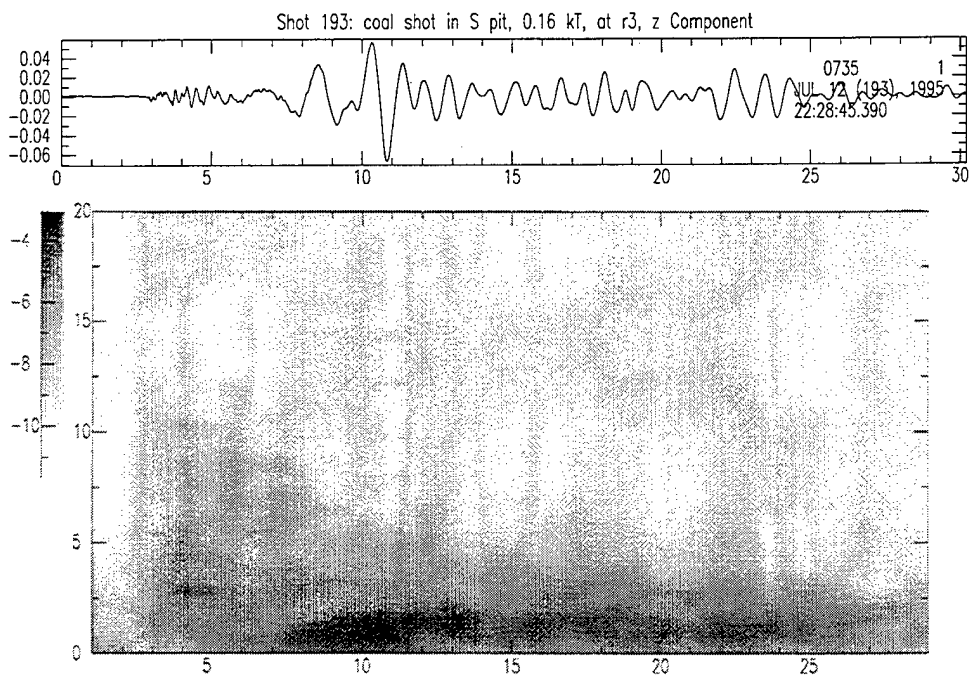
Figure 9. Seismogram and spectrogram (vertical component) for coal shot 193 in the south pit, recorded at station R3.

The ratio of shear to compressional energy in a regional signal is a feature often studied as a discriminant. In the following, we examine this ratio in the Black Thunder near field data. Again, we focus on blasts occurring in the south pit, recorded at station R3. Seismograms for three cast blasts are shown in Figure 10, and for three coal shots in Figure 11.

Time (sec)

Station r3   Shot Type: cast

9.9e-02   174
1.00   S Pit

2.4e-01   167
4.41   S Pit

1.3e-01   206
1.55   S Pit

z.vpz component

Filter: none

Time (sec)
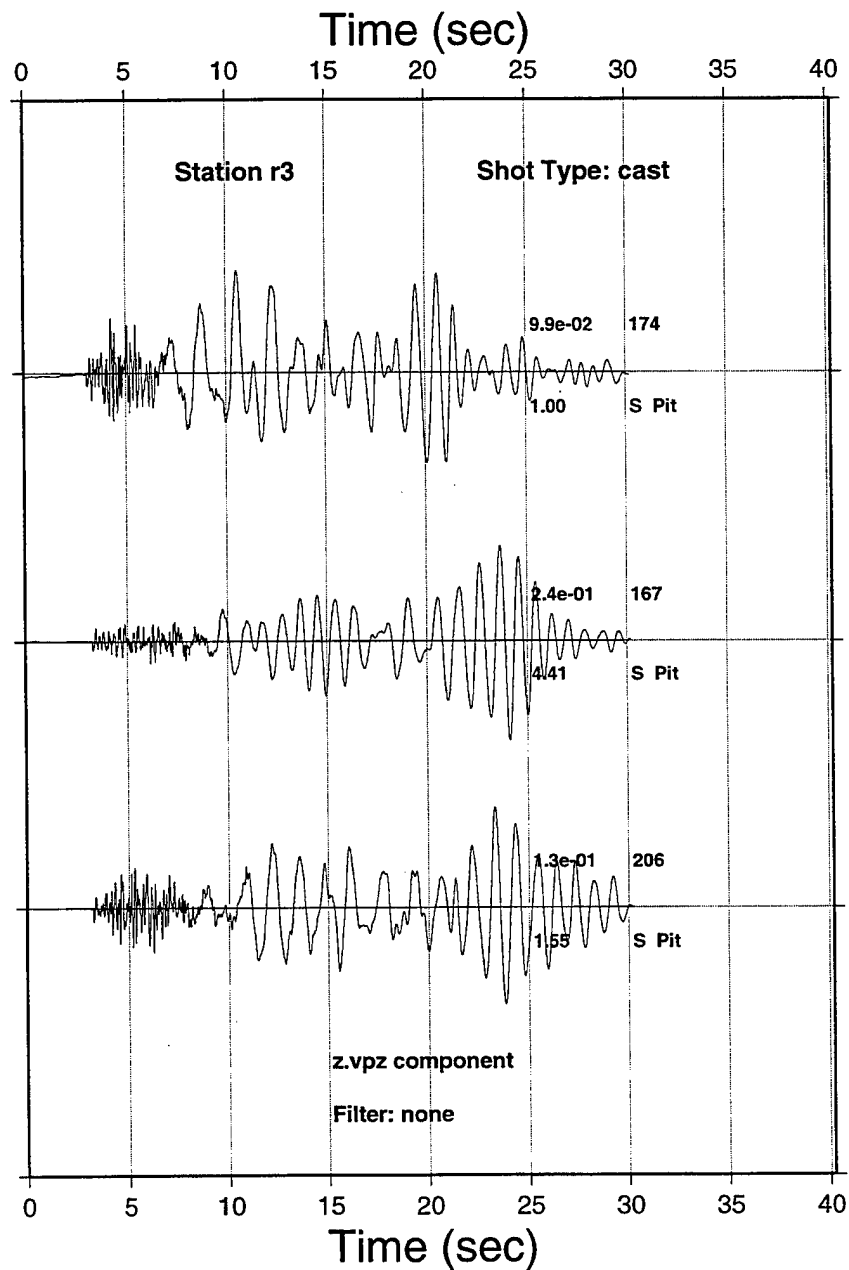
Figure 10. Vertical seismograms for three cast blasts in the south pit, recorded at R3.
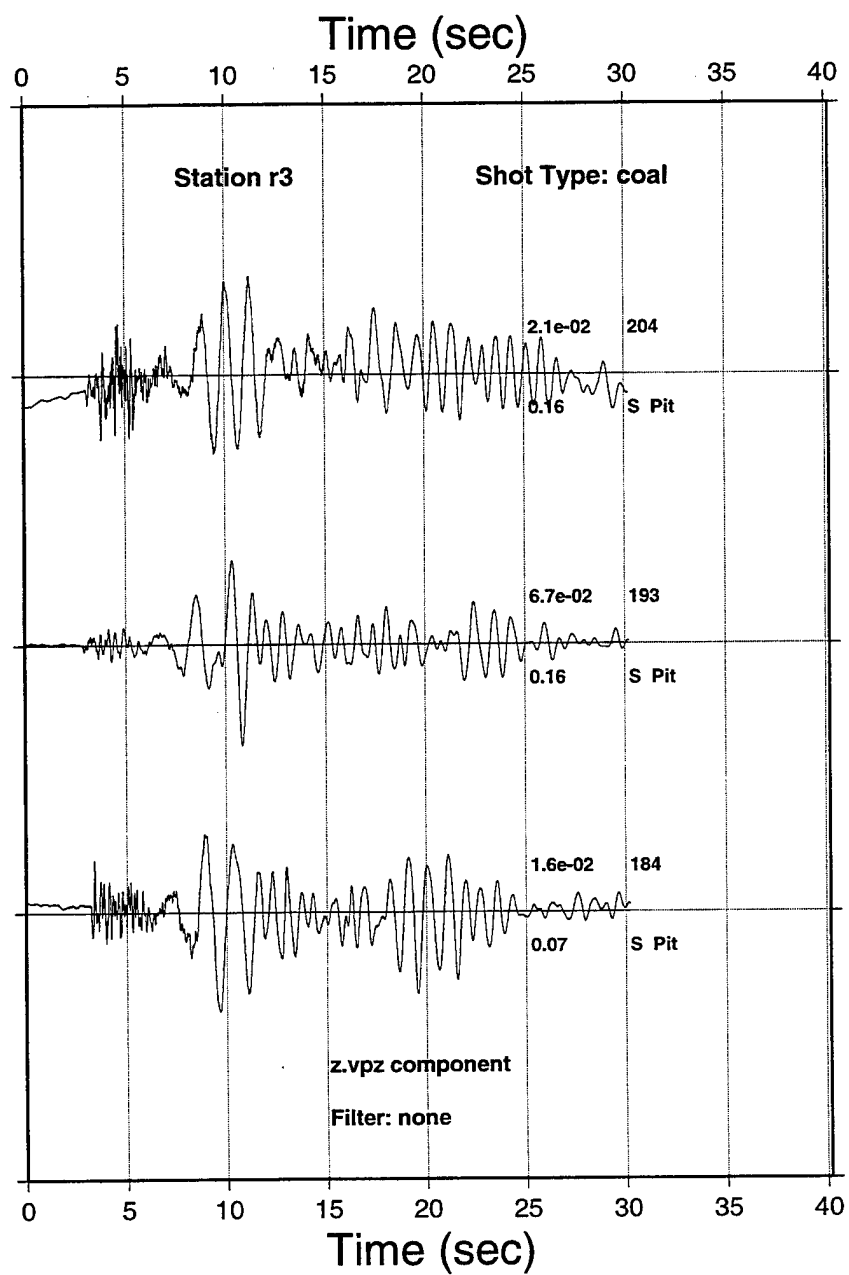
Figure 11. Vertical seismograms for three coal shots in the south pit, recorded at R3.

Visual inspection of the records from the different shot types indicates no apparent differences between the shot types. Recall that the early arriving, high frequency energy is associated with P waves and later, lower frequency energy is surface waves. We use as a measure of P and S energy the amplitudes of the early and late, respectively, signals. Figure 12 shows narrow band envelope functions of the vertical component for the cast shots at two center frequencies, 2 and 8 Hz. In each case, the bandwidth of the filter is 2 Hz. Also on the figure are S/P ratios computed from ratio of the peak S envelope at 2 Hz to the P envelope at 8 Hz. There is a factor of 5 variation in this parameter, with an average value of about 20.
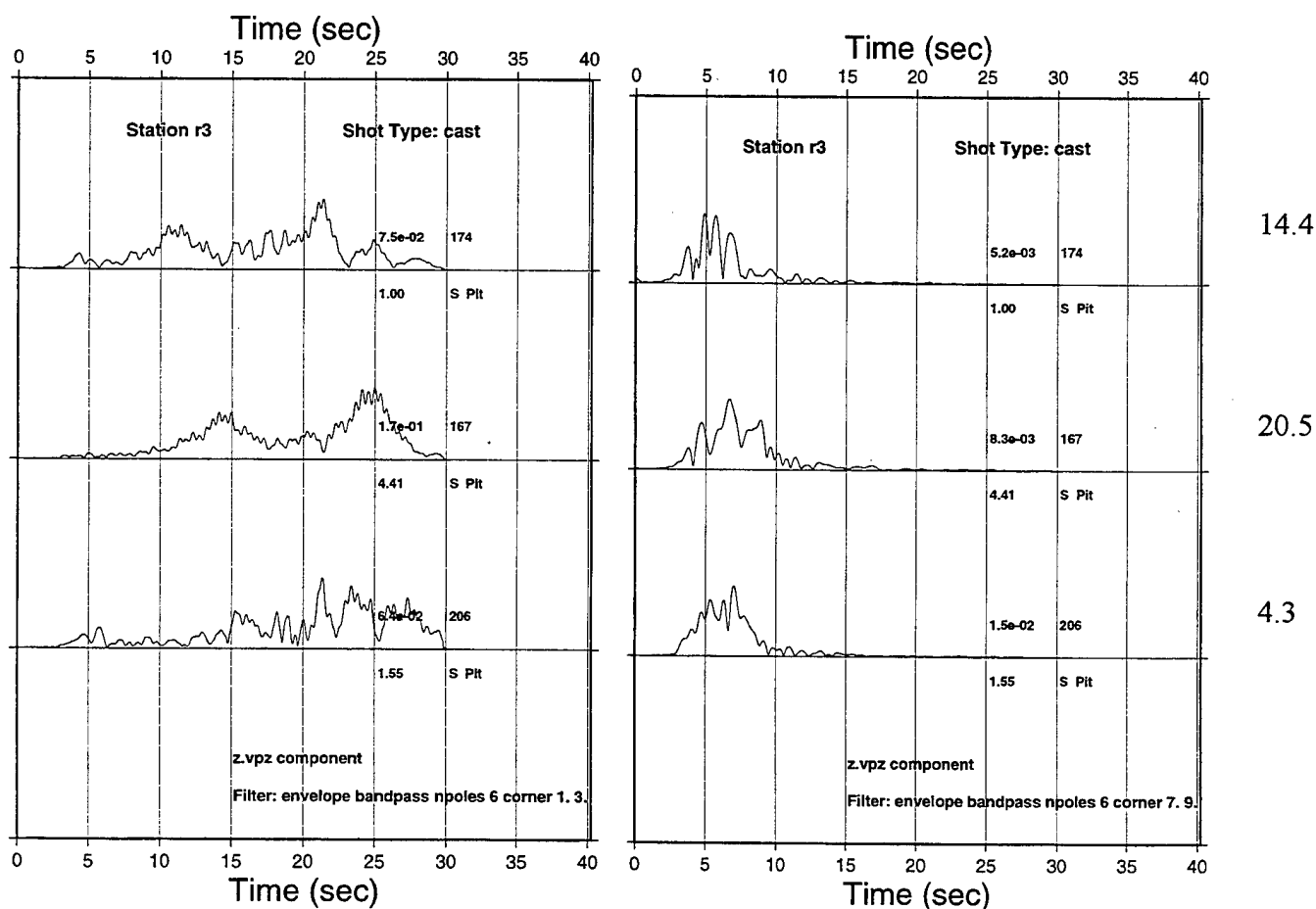
Figure 12.   Narrow band envelope functions and S/P ratios (vertical component) for cast shots in the south pit at station R3.

18

A comparable plot for the coal shots is shown in Figure 13. The average S/P ratio is about 18, and the minimum and maximum values are similar to those from the cast blast. It appears that in the near field there are no significant differences in S/P excitation between the two source types. This comment applies to the radial and tangential components as well.
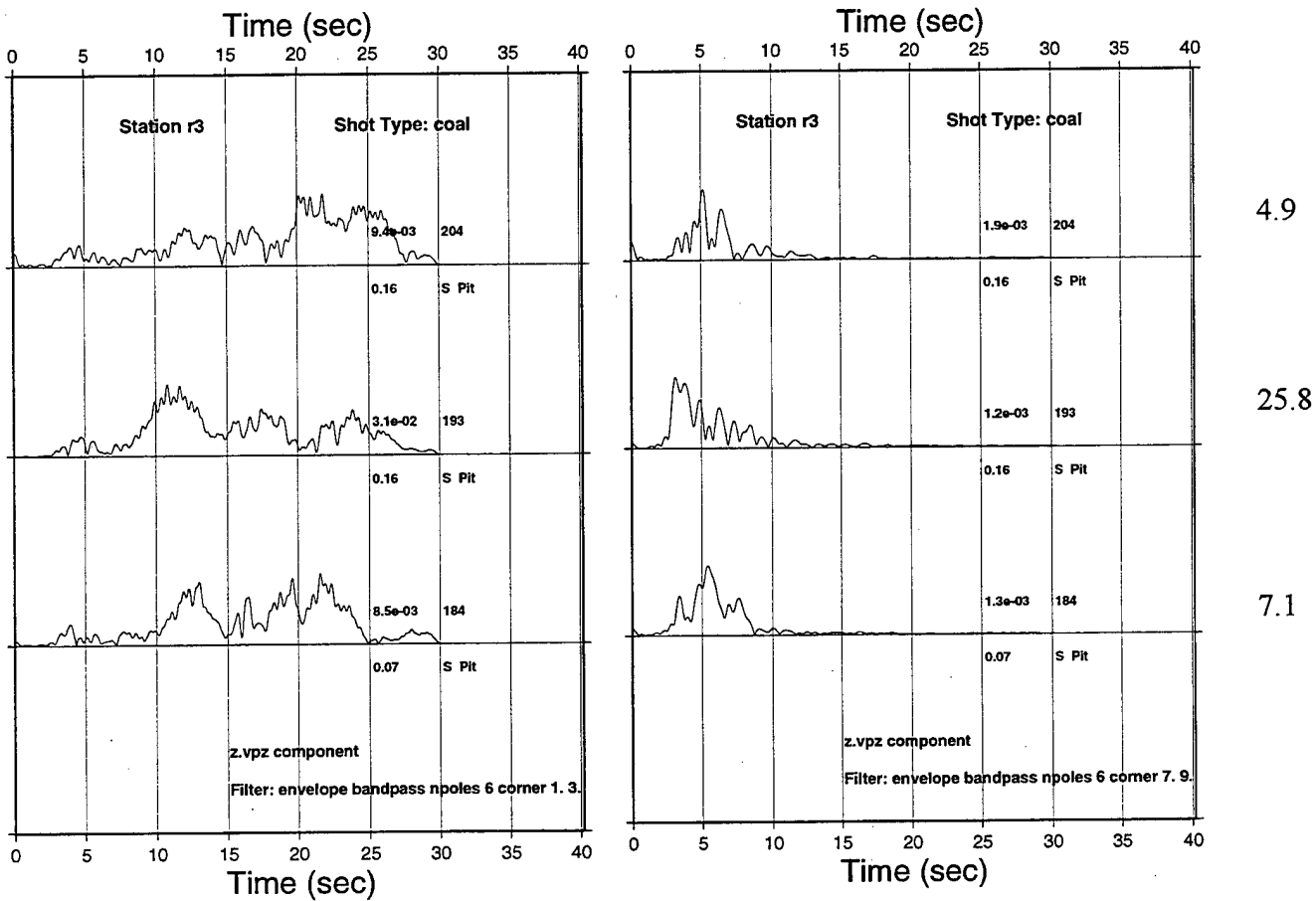
Figure 13. Narrow band envelope functions and S/P ratios (vertical component) for coal shots in the south pit at station R3.

In Figure 14, we compare three coal shots in the south pit and one in the west pit at station R3 (see Figure 1). The distance from the west pit shot to R3 (10.2 km) is slightly closer than the south pit shots (about 13 km), and the azimuth is closer to north. Recall that the west pit is aligned north-south while the south pit is aligned east-west. The differences between shots within the south pit are comparable to the differences between shots in the two pits.

19
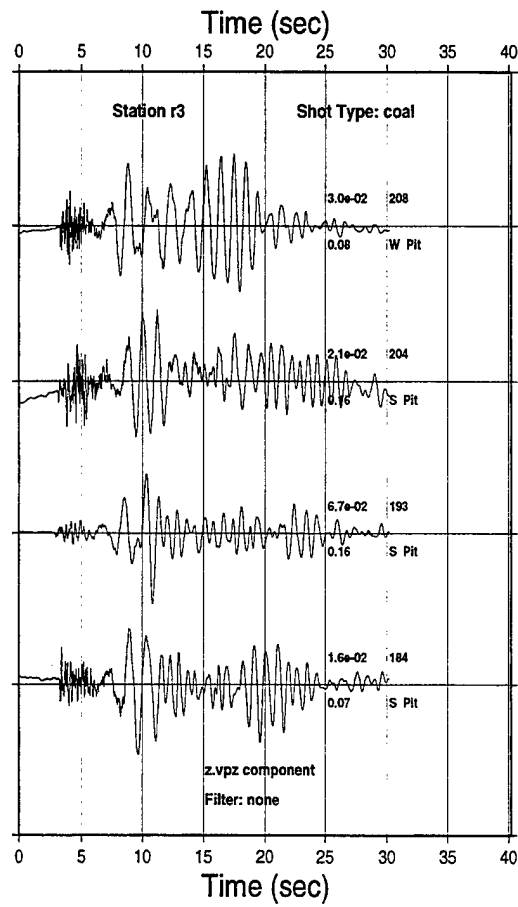
Figure 14. Vertical component seismograms from three coal shots in the south pit and one in the west pit at station R3.

In addition to S/P ratios, a feature often proposed as a discriminant is the spectral slope. In Table 3, we show spectral slopes of the surface waves for the shots in this data set. The slopes were computed by linear regression of the log of the amplitude spectrum versus log of frequency for frequencies above 1 Hz. The spectra are shown in Figure 15. The surface waves were chosen since their character is most likely to be indicative of Lg excitation. Three of the cast blasts have nearly the same slope, -1.6, but one shot (199) has a slope of -1.8. The coal shots have a greater scatter, ranging from -1 to -2.1, a range which brackets the cast blasts. The slope of the simultaneous coal shot lies in the ranges of both other shot types.

Table 3. Spectral slopes of the surface waves for the shots in this data set. The slopes were computed by linear regression of the log of the amplitude spectrum versus log of frequency for frequencies above 1 Hz

cast	
167	-1.59239
174	-1.55655
199	-1.83844
206	-1.57163
coal	
171	-1.71765
184	-1.62791
193	-2.10487
204	-1.20198
208	-0.975225
simultaneous	
236	-1.80378
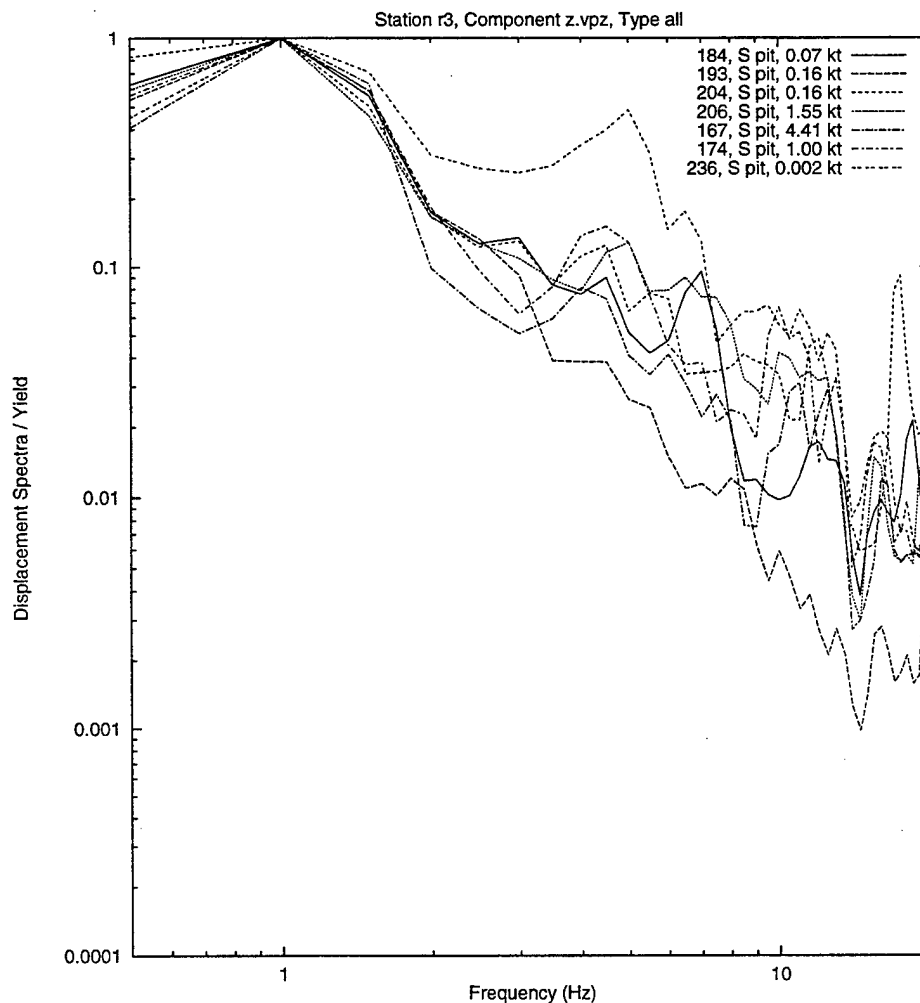
Figure 15. Spectral amplitudes of the surface waves for the shots recorded at station R3. Values have been normalized to the value at 1 Hz for each spectrum.

In summary, with regard to S/P ratios, spectral slopes and seismogram character, one cannot distinguish shot type or pit from these near-field data. In addition, we cannot determine whether this is characteristic of shots in the Black Thunder mine or whether this is characteristic of near-field data.

5.1 Inference of Source Structure, Comparison with Synthetics.

As mentioned above, signals at Black Thunder are strongly influenced by propagation effects. We have no independent information on earth structure or propagation properties, but we do have drilling reports. Thus, we adopted a strategy of using the source model proposed by Barker et al., (1993a) with the parameters fixed by drilling reports and then varying propagation properties in order to match synthetic seismograms. This source model was used to interpret the Texas Chemline Quarry data in Bonner et al. (1996) and was the basis for the analyses of Black Thunder signals recorded at regional distances at PDAR by Anandakrishnan et al. (1997). The model consists of an explosive component and a spall or mass movement component. We focused on station R3, which is 11.6 km NNW of shot 236, the simultaneous coal shot (see Figure 1). This station was chosen since there are recordings there of several different source types and the range is great enough for seismic phases to separate in time.

Since only nominal shot times are available, structure could not be obtained from absolute travel times. As a first cut at identifying seismic phases, we made experiments using our surface wave modal program SYNSRF and earth structures appropriate to the geology (low velocity unconsolidated surficial sediments with a shallow coal seam). These calculations show that the signals which dominate the later parts of the records are fundamental and a few higher mode surface waves. We applied narrow-band filter analyses to the data to infer dispersion properties but interference between modes made interpretation unreliable. We had no formal inversion scheme that seemed applicable, so we opted for a parameter-space search of an earth model. We used the wavenumber integration code PROSE to compute propagation Green's functions which included body and surface waves for layered structures. Since it was found that the synthetic seismograms were sensitive to structure to a depth of about 200 m, we restricted our parameter search to those depths. The procedure was to vary the velocities in a model in which the upper 4 layers each had a thickness of 50 m, compute synthetic seismograms and compare the results to data. The shear velocities β of the layers were varied at 100 m/sec increments from 200 m/sec to 1000 m/sec, with the condition that the velocities increase with depth. The computed seismograms were most sensitive to β and Q_β, and relatively insensitive to compressional velocity α and Q_α, so the compressional values were set to be a multiple of the shear values. The procedure was repeated for several families of values of Q_β. In spite of the relative insensitivity to α, it was possible to infer that the Poisson's ratio is high.

We began with the simultaneously detonated coal shot (236) since it should have had the most impulsive source function and least amount of mass movement relative to the cast blasts and the other (ripple-fired) coal shots. The simultaneously detonated coal shot is modeled as a grid of 5 rows (parallel to the shot face) by 3 columns of charges of equal yield for a total yield of 40,000 pounds. Charges are spaced at 10 m intervals. The purpose of a coal shot is to bulk the material and a significant amount of movement of the overburden is observed. Thus, a signal due to spall is added to a signal from the explosive detonation for each charge. The initial vertical velocity of the spalled material is assumed to be 3.5 m/sec. The tangential motion at station R3 is observed to be comparable to the

23

radial motion, so we further assume that the spall involves horizontal movement as well as vertical. The formulation for combining the spall and explosive time functions with the Green's functions is given by Barker *et al.* (1993b).

The Green's functions were convolved with the source functions and the results compared visually to the observations. The diagnostic features used to judge the goodness of fit were signal duration and relative timing and amplitude of apparent phases on the records. Particular attention was paid to the start and end times of the surface wave trains. The structure derived in this manner is shown in Figure 16. The structure in the surficial 100 m was verified by borehole measurements made recently in the vicinity (R. Nigbor, Agbabian Associates, personal communication).
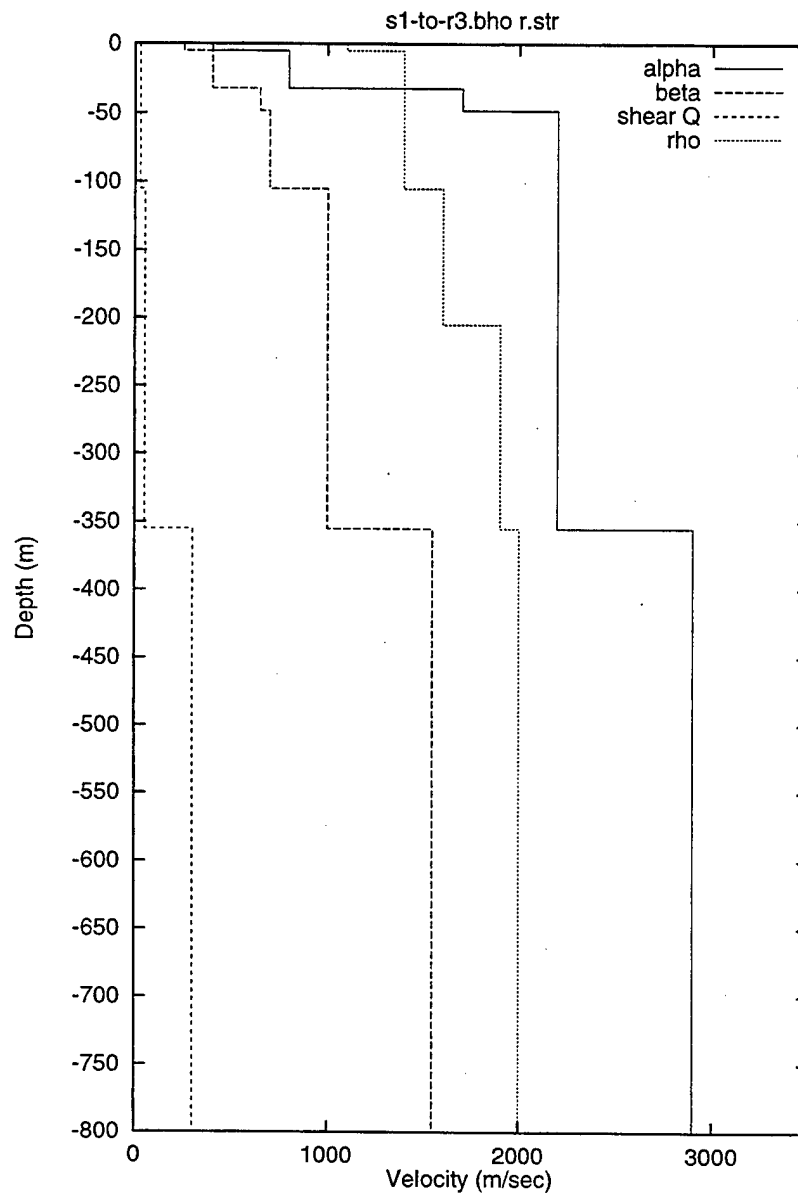

Figure 16. Earth structure used in the calculation of synthetic seismograms.

24

Figure 17 shows the explosive and spall or mass movement contributions to the synthetic vertical motion at R3 for the shot 174 source model. The peak motion, which is associated with the surface waves, from the explosive component is about 3 times the peak from the spall. The ratio of S to P motion due to the spall component exceeds 10 while the S/P ratio of the explosive part is about 3. The surface waves from the explosive component are largest late in the record (from 17 to 25 seconds), while those from the spall component arrive during the span from 10 to 25 seconds.
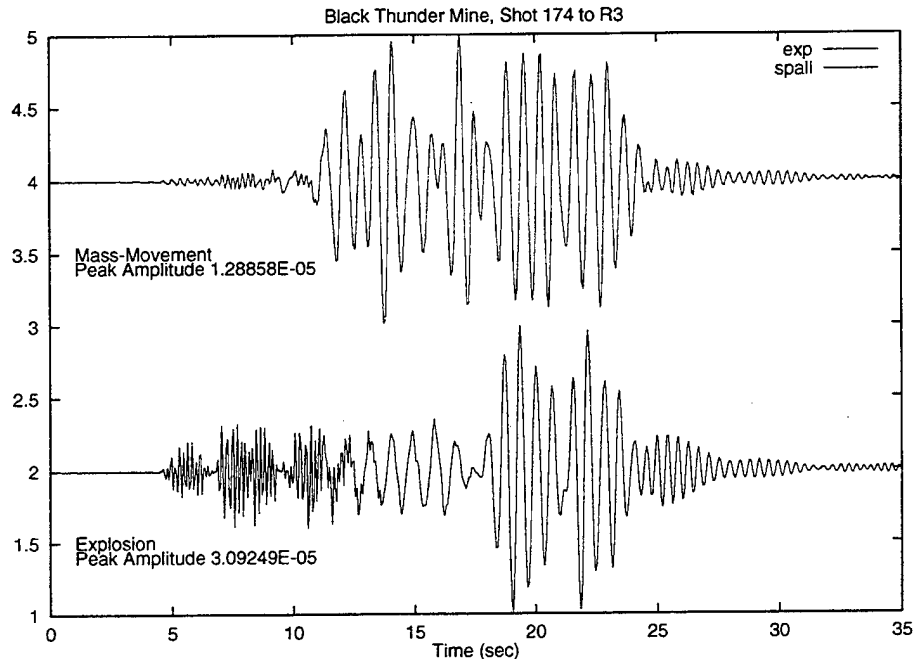
Figure 17. The spall and explosive contributions to the synthetic vertical motion at R3 for the shot 174 source model. The signals are globally scaled, with the peak motions indicated on the plot. The upper trace is the spall contribution and the lower trace is the explosive contribution.

Tangential synthetic and observed seismograms from coal shot 236 at R3 are compared in Figure 18. The data provided to us had been processed to remove the instrument response, which introduced a long period component, which detracted from this analysis. Thus, we have high pass filtered the time series at a corner frequency of 1 Hz to remove long period artifacts. The peak ground displacements from the synthetic record are within a factor of three of the observed record. The duration is matched fairly well, except for a small wave train after 25 sec. There is a phasing in the observed record that is roughly duplicated by the synthetic.

Figure 18. Tangential synthetic (upper) and observed (lower) displacement seismograms from coal shot 236 at R3. Peak displacements are indicated by the numbers below the time series (at the 30 sec line).

The corresponding vertical motions from the coal shot at R3 are shown in Figure 19. The synthetic vertical component seismograms include the explosive and vertical spall contributions. As with the tangential motions, the calcu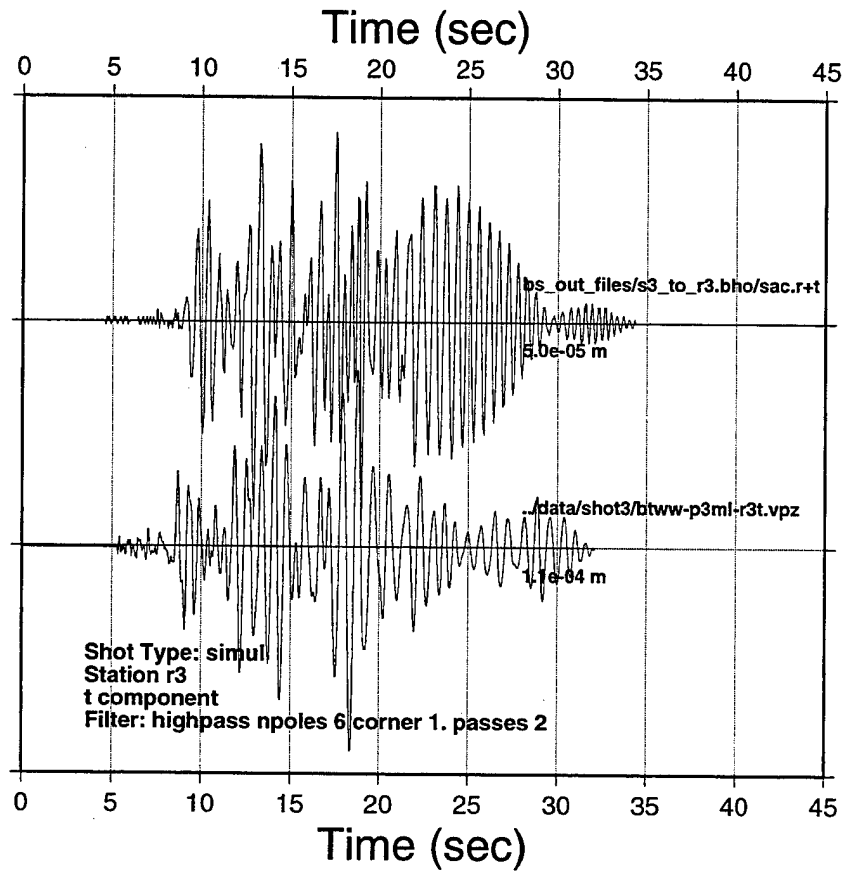lated peak displacement is about one third the observed value and the amplitude of the calculated signal arriving after 20 seconds is too small. To increase the amplitude of this late arriving energy, we tried increasing the values of Q in the surficial layers, but this did not produce the desired effect. We were unable to reproduce this late signal strength with reasonable values of seismic velocity in the shallow layers at this receiver location or at the closer station R2. Two explanations for this are (1) non-plane-layer propagation and (2) the actual source duration was longer than designed. A more complicated earth structure would not be expected to increase signal strength at both distances, so we hypothesize that the signal duration was longer than designed. The large high-frequency signal at the start of the observed record is probably caused by charges that did not fire according to the planned intervals. Because the calculated amplitudes are smaller than observed for both tangential and vertical components, we conclude that explosive coupling is higher than in the model and that there is significant conversion of P to S energy from the explosives. The mode conversion is consistent with calculations showing the effect of the quarry bench (Barker *et al.*, 1993b, McLaughlin *et al.*, 1994 and McLaughlin *et al.*, 1996).
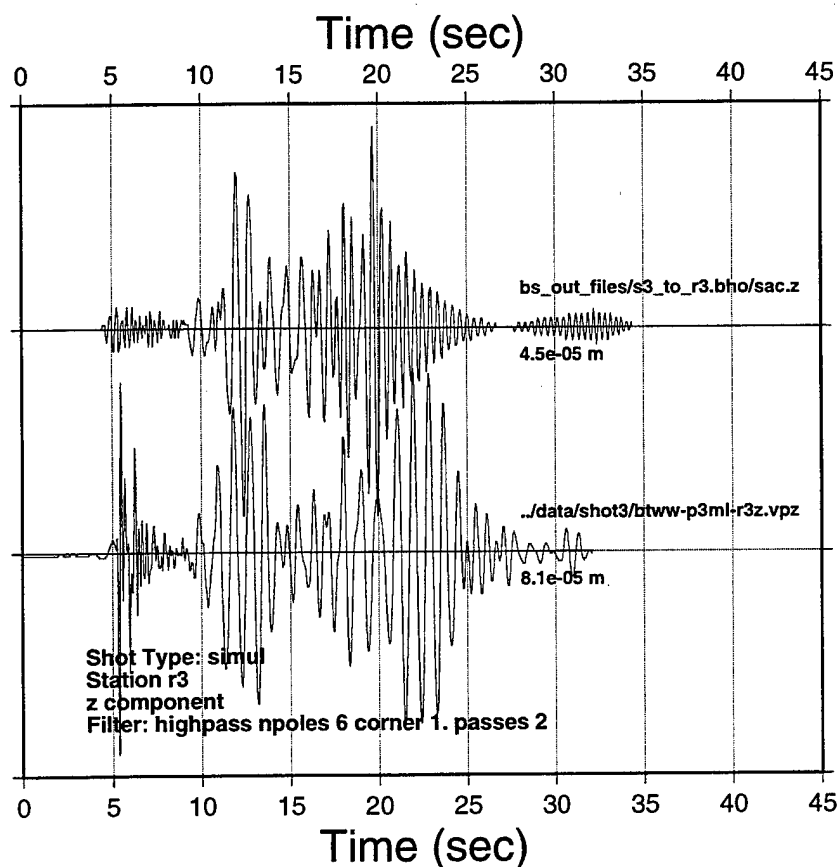
Figure 19. Vertical synthetic (upper) and observed (lower) displacement seismograms from coal shot 236 at R3. Peak displacements are indicated by the numbers below the time series (at the 30 sec line).

Additionally, the two large cast blasts were modeled. Cast blast 167 was modeled using 8 rows by 88 columns of charges, again at 10 m intervals. Time intervals followed the shot log design values which were that charges within columns were detonated at 35 ms intervals while rows were fired at times 125, 300, 500, 700, 900, 1200 and 1400 ms after the first row (Craig Pearson, LANL, personal communication). The initial velocity of the spalled material was assumed to be 3.5 m/sec with an initial angle of 30^0 from the horizontal. The shot was designed to throw material to the NE, which we assume to have occurred. Figure 20 shows tangential synthetic and observed seismograms from cast blast 167 at R3. The peak displacement is about one-fifth the observed value. The duration of the signals is longer than the coal shot 236, consistent with the increased duration of the blasting sequence. As with the coal shot, the relative amplitude of the late arriving signal (after 25 sec) is too small on the synthetic compared with the observed.

The vertical motions for cast blast 167 are shown in Figure 21. Again, the calculated peak amplitude and relative amplitude of late-arriving energy are less than observed. We conclude that we can achieve better agreement with observations by (1) increasing the source duration and (2) include P to S conversion from the explosive component of the source.

27

Time (sec)

bs_out_files/s1_to_r3.bho/sac.r+t

4.5e-05 m

../data/shot1/btww-p1ml-r3t.vpz

2.1e-04 m

Shot Type: cast
Station r3
t component
Filter: highpass npoles 6 corner 1. passes 2

Time (sec)

Figure 20. Tangential synthetic (upper) and observed (lower) displacement seismograms from cast blast 167 at R3. Peak displacements are indicated by the numbers below the time series (at the 30 sec line).

Time (sec)

0 5 10 15 20 25 30 35 40 45

bs_out_files/s1_to_r3.bho/sac.z

3.5e-05 m

../data/shot1/btww-p1ml-r3z.vpz

2.2e-04 m

Shot Type: cast
Station r3
z component
Filter: highpass npoles 6 corner 1. passes 2
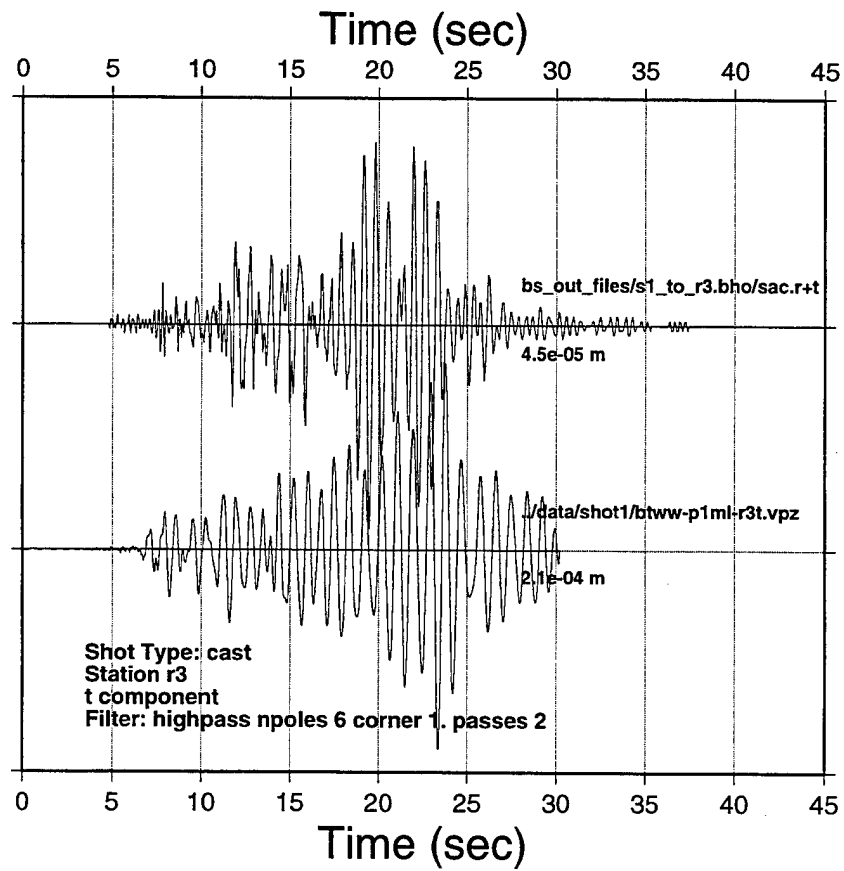
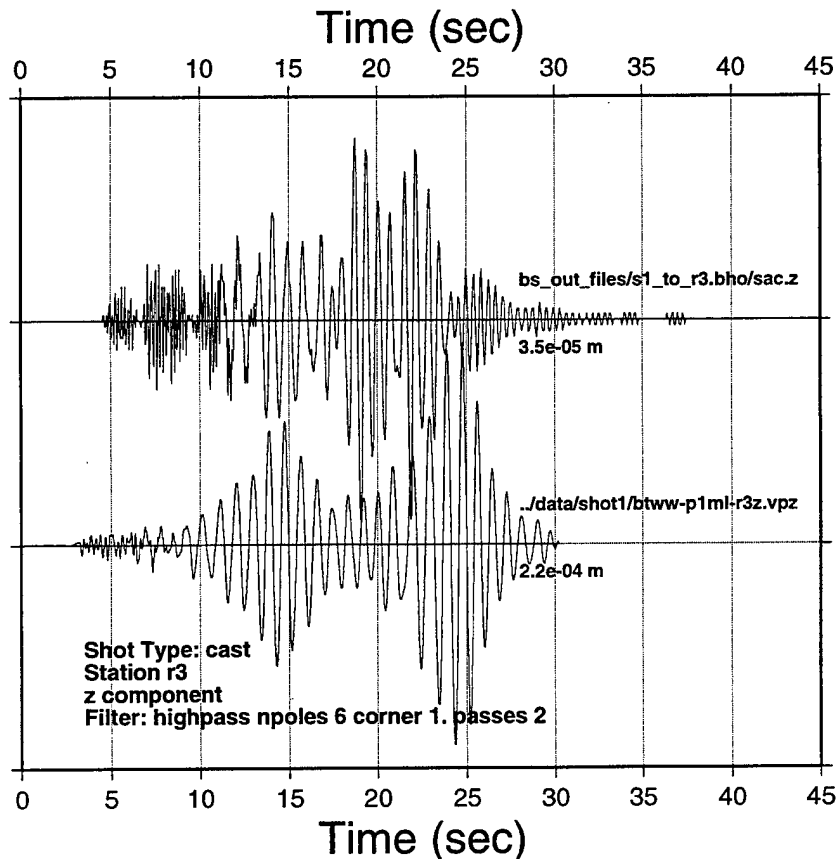0 5 10 15 20 25 30 35 40 45

Time (sec)

Figure 21. Vertical synthetic (upper) and observed (lower) displacement seismograms from cast blast 167 at R3. Peak displacements are indicated by the numbers below the time series (at the 30 sec line).

Consider next the other cast blast in this data set, shot 174. Recall that this shot was located near 167, but threw material to the NW. Cast blast 174 was modeled using 7 rows by 30 columns of charges with 10 m spacing. Time intervals followed the shot log design values which were that charges within columns were detonated at 35 ms intervals while rows were fired at times 125, 300, 500, 700, 900 and 1200 ms after the first row. Figures 22 and 23 show observed and synthetic tangential and vertical motions, respectively.

It is interesting to compare Figures 20 and 21 for shot 167 with Figures 22 and 23 for shot 174. Although the surface waves on the vertical components (Figures 20 and 22) are similar, the body waves from these shots show that signals from the same source type on the same face of the same pit can be quite different.

Time (sec)

0   5   10   15   20   25   30   35   40   45

bs_out_files/s2_to_r3.bho/sac.r+t

3.3e-05 m

../data/shot2/btww-p2ml-r3t.vpz

9.8e-05 m

Shot Type: cast
Station r3
t component
Filter: highpass npoles 6 corner 1. passes 2

0   5   10   15   20   25   30   35   40   45

Time (sec)

Figure 22. Tangential synthetic (upper) and observed (lower) displacement seismograms from cast blast 174 at R3. Peak displacements are indicated by the numbers below the time series (at the 30 sec line).
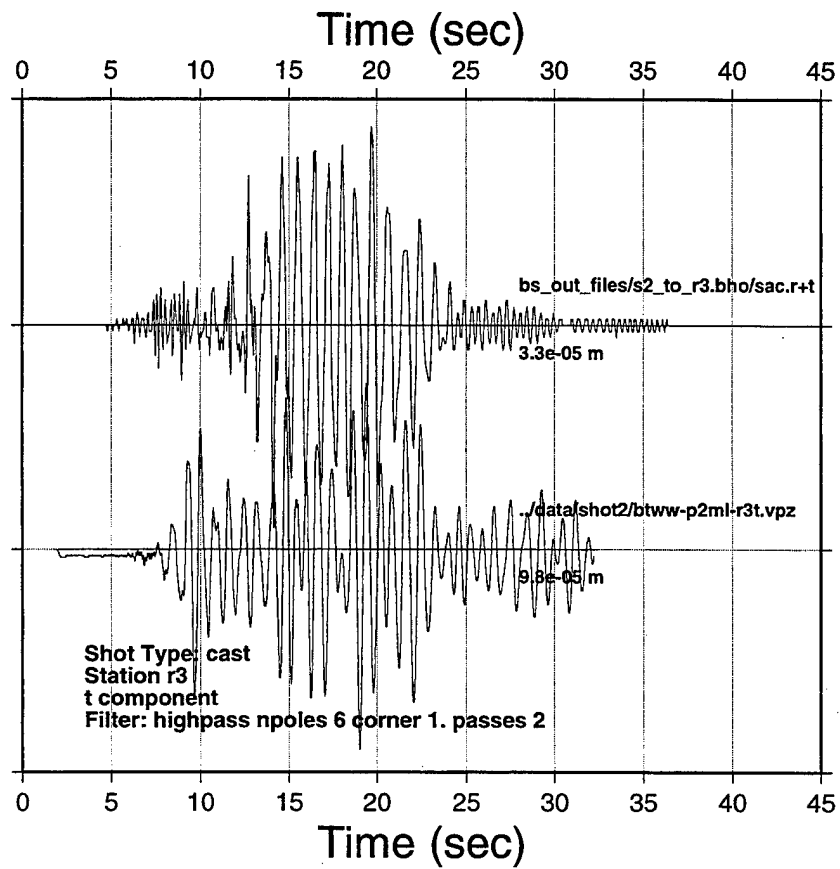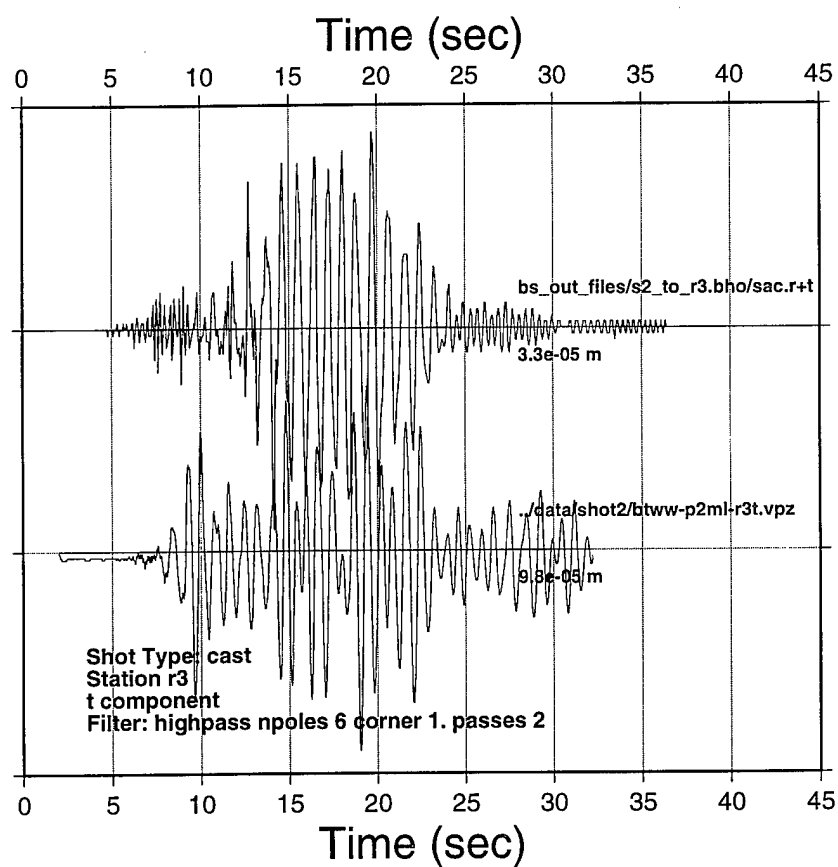
Figure 23. Vertical synthetic (upper) and observed (lower) displacement seismograms from cast blast 174 at R3. Peak displacements are indicated by the numbers below the time series (at the 30 sec line).

31

6.0 Black Thunder Mine Series: Regional Data

In addition to studies of the near-field data described above, we have begun analyses of near-regional data presented by Hedlin et al., (1996). In the summer of 1996, IGPP/UCSD deployed five seismometers at ranges between 100 and 200 km from the Black Thunder mine, which augment the permanent regional stations RSSD and PDAR (Figure 24). Hedlin et al. (1996) recorded three large blasts, two in the South Pit (shots 214 and 215) and one in the North Pit (shot 201). During South Pit shot 215, a large fraction of the holes detonated simultaneously (unintentionally). Data from these shots were provided to us by Dr. Hedlin.
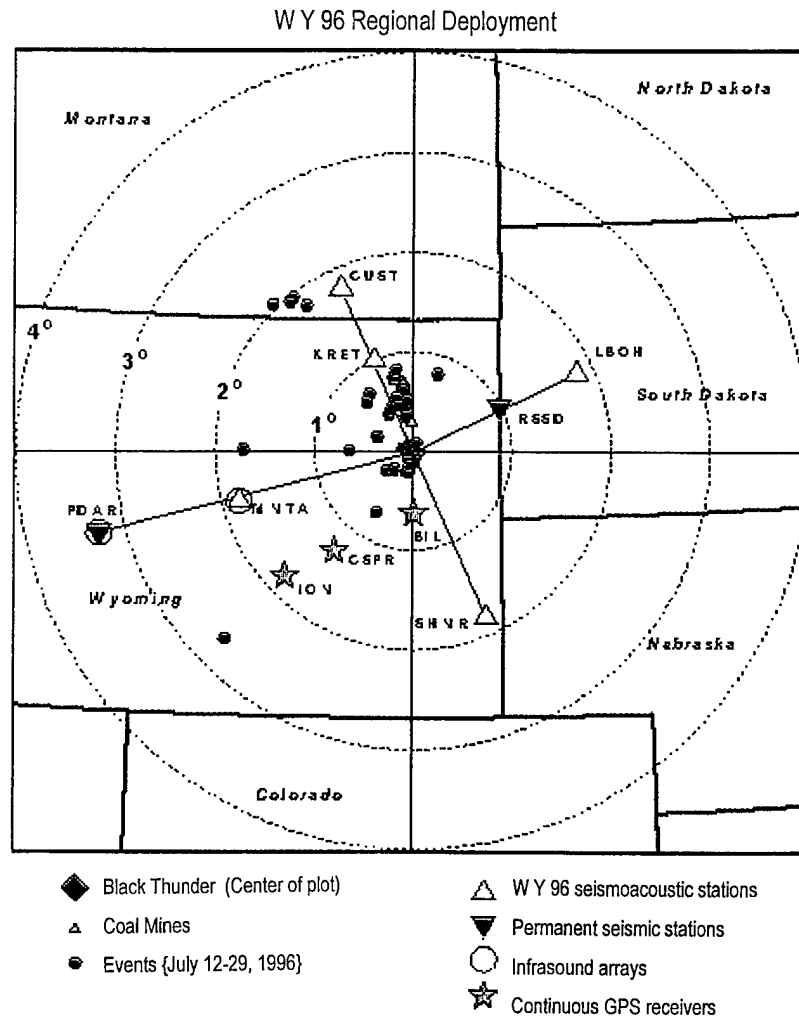

Figure 24. Map showing Black Thunder mine and stations deployed by Hedlin et al. (1996).

32

To isolate source properties, we inferred path properties to these sites. The signals have good Rayleigh waves, so we extracted dispersion curves and inverted them for earth structure using signals from three shots. Figure 25 shows the shear wave structures derived for each site using shot 201. The results are comparable for the other shots.

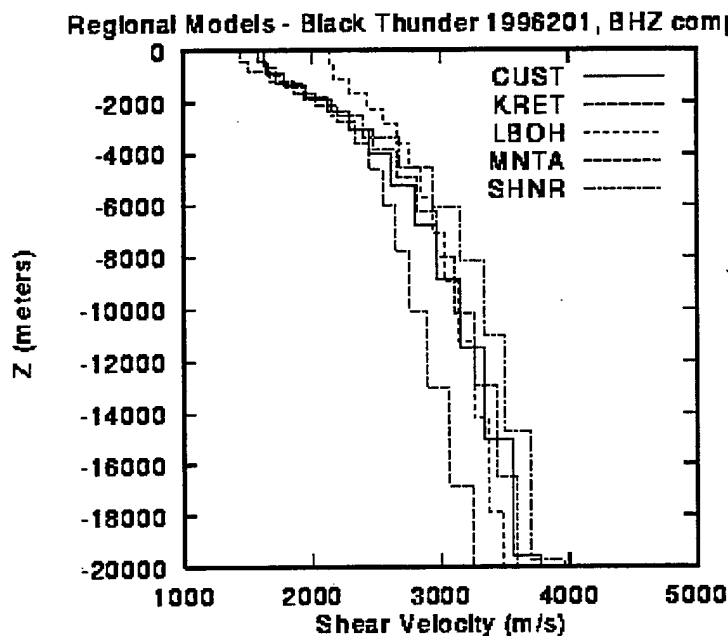**Regional Models - Black Thunder 1996201, BHZ component**

Figure 25. Shear velocity structure at four sites from the shot on Julian day 1996201.

The models are quite consistent, with the exception of LBOH. These sites are all within the Powder River and Wind River Basins, except LBOH. Signals to LBOH are perhaps different because they must cross the Black Hills pluton.

Figures 26 a and b show spectra at stations MNTA and SHNR. The spectra have been corrected for propagation by using Rayleigh wave phase velocities as phase matched filters. At MNTA, the spectra from shots 214 and 215 (in the South Pit) are quite similar, while shot 201 (in the North Pit) is different from them. This would indicate that in this bandwidth the shot location (i.e., in which pit it occurs) influences the spectrum more than the firing pattern. This is the case at station SHNR below 0.4 Hz, but not as convincingly above 0.4 Hz.

To emphasize the South Pit spectra relative to the North Pit, the spectra for shots 214 and 215, divided by the corrected spectrum of shot 201, are shown in Figures 27 a and b for station MNTA and SHNR. Again, these figures indicate that source location has a stronger effect on amplitude than firing pattern at low frequencies.
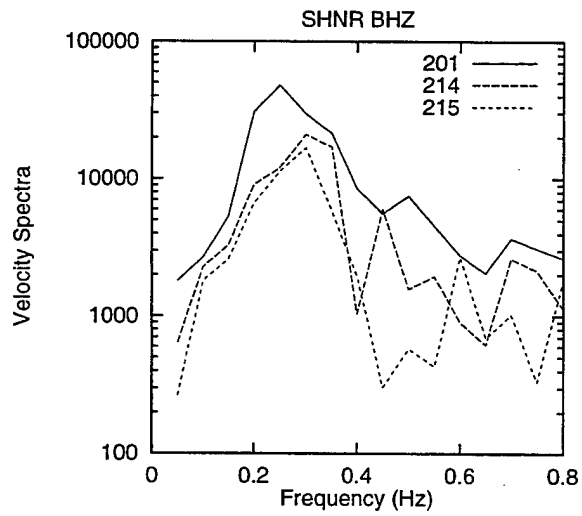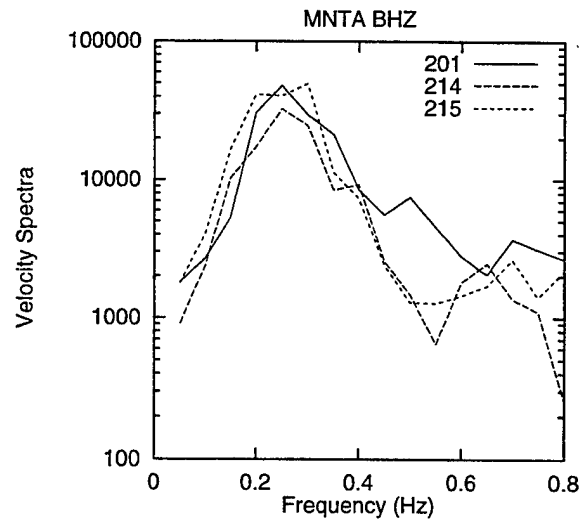
Figures 26 a and b. Log of spectra at stations MNTA (top) and SHNR (bottom). The spectra have been corrected for propagation by using Rayleigh wave phase velocities as phase matched filters.

Phase Matched Filter Derived Rayleigh Spectra, MNTA BHZ

Phase Matched Filter Derived Rayleigh Spectra, SHNR BHZ
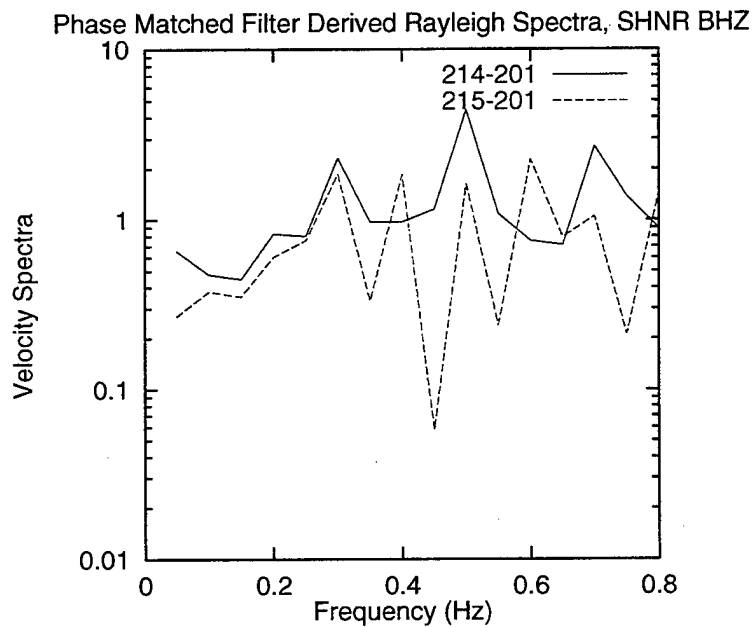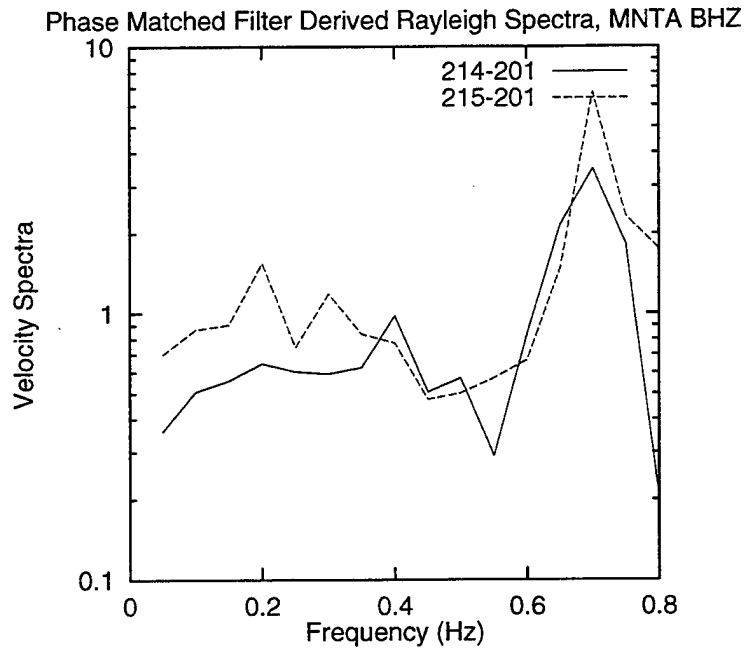
Figures 27 a and b. Log of spectra of South Pit shots 214 and 215 relative to North pit shot 201, at stations MNTA (top) and SHNR (bottom).

Radiation patterns of path corrected spectral amplitudes at 0.8 Hz for shots 201, 214 and 215 are shown in Figures 28, a to c. For this limited azimuthal coverage, it can be said that the radiation patterns for each shot are similar. For each shot, the peak motion is observed to the southwest at station MNTA, with intermediate values to the northwest and southeast. For this set of events at this frequency, shot location and firing pattern do not appear to affect Rayleigh wave radiation patterns. Bonner *et al.* (1996) observed variations in Rayleigh wave amplitudes in signals from a Texas quarry, but this was at higher frequencies (at which they could infer structure since their stations were much closer).

Shot 214
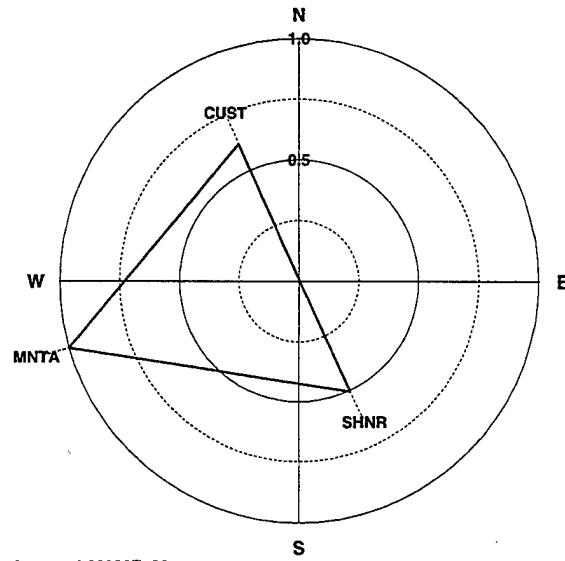
Amax = 1.60000E+23

Shot 201
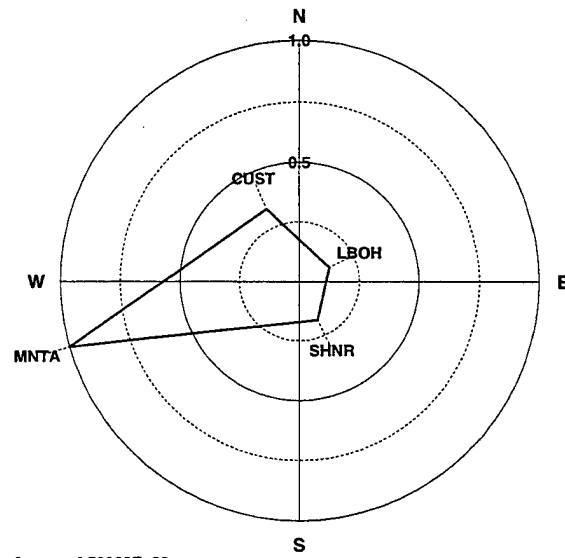
Amax = 4.50000E+23

Shot 215

Amax = 2.30000E+23

Figure 28, a ,b,c. Radiation patterns of path corrected spectral amplitudes at 0.8 Hz for shots 201, 214 and 215.

7.0 Conclusions

We make the following conclusions.

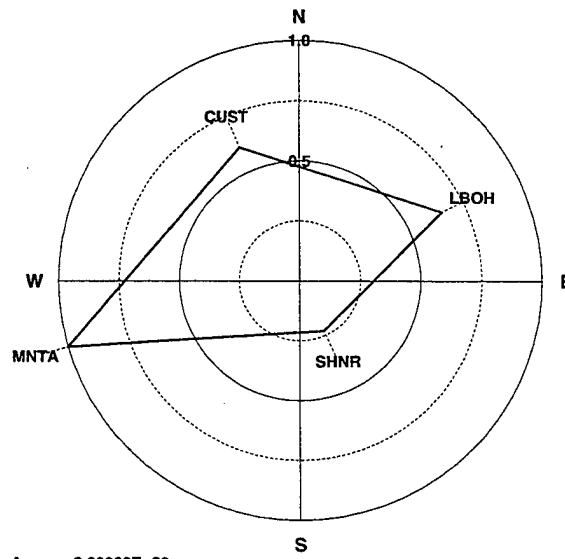1. Ripple firing effectively low pass filters the signals, in agreement with previous studies. Since for the near-field signals at Black Thunder, the observed high frequency components of the signals are associated with P waves and the lower frequency signals are associated with surface waves (dominated by shear motion), ripple firing has the indirect effect of increasing the S/P ratio in the seismograms.

2. We observe no consistent differences between motions from cast blasts and ripple-fired coal shots. In our previous numerical studies under this contract (Barker et al., 1997) and in field studies (Bonner et al. 1996), azimuthal variations due to throw or strike of the bench were predicted and observed. We observe no differences between cast shots at the Black Thunder mine in which the throw or strike of the bench is different. We examined differences in seismogram character, S/P ratio and spectral slope. The lack of differences is due to the dominance of ground motion caused by explosions relative to that caused by mass movement, which is in turn is due to relative source coupling or propagation. Since differences in mass movement are the primary differences in the source mechanisms between coal and cast blasts, the dominance of the explosion component obscures the source mechanism.

3. Vertical and tangential near field ground motions (corrected for site response) from cast blasts are strongly enhanced normal to the bench in the direction of unmined land. We have no azimuthal coverage of a coal shot.

4. In contrast to the results of our previous studies in Texas (Barker et al., 1997, Bonner et al. 1996), near-regional ground motions (corrected for path) show no azimuthal dependence on shot orientation.

8.0 References

Anandakrishnan, S., S.R. Taylor and B.W. Stump, "Quantification and characterization of Regional Seismic Signals from Cast Blasting in Mines: a Linear Elastic Model," *Geophys. J. Intl.*, **131**(1), 45-60.

Barker, T.G., K.L. McLaughlin and J.L. Stevens (1993a), "Numerical Simulation of Quarry Blast Sources," S-CUBED Technical Report to Phillips Laboratory, Kirtland AFB, SSS-TR-93-13859. ADA 265517

Barker, T.G., K.L. McLaughlin, J.L. Stevens and S.M. Day (1993b), "Numerical Models of Quarry Blast Sources: the Effects of the Bench," S-CUBED Semiannual Report to Phillips Laboratory, Kirtland AFB, SSS-TR-93-13915. ADA 265370

Barker, T.G., K.L. McLaughlin J.L. Stevens (1996), "Physical Mechanisms of Quarry Blast Sources," *Proceedings of the 18th Annual Seismic Research Symposium on Monitoring a Comprehensive Test Ban Treaty*, edited by J.F. Lewkowicz, J.M. McPhetres and D.T. Reiter, Annapolis MD, PL-TR-96-2153, ADA313692.

Barker, T.G., K.L. McLaughlin, J. L. Bonner (1997), "Physical Mechanisms of Quarry Blast Sources," Maxwell Technologies Scientific Report to Department of Energy and Phillips Laboratory, MFD-TR-97-15695.

Bonner, J.L. and T. Goforth (1995), "Characteristics of Rg Waves Recorded from Quarry Blasts," *Bull. Seism. Soc. Am*, **85**, pp. 1232-1235.

Bonner, J.L., E. Herrin and T. Goforth (1996), "Azimuthal Variation of Rg Energy in Central Texas," *Geophys. Res. Lett.*, **67**, (4), pp. 43-56.

Day, S.M. and K.L. McLaughlin (1991), "Seismic Source Representations for Spall," *Bull. Seism. Soc. Am.*, **81**, pp. 191-201.

Delitsyne, L. (1996), "Generation of Shear Waves from Quarries from Near-Regional Data," *Seism. Res. Lett..* **67**, (2), p. 36.

Hedlin, M.A.H., F.L. Vernon, J.B. Minster and J.A. Orcutt (1996), "Experiments in Regional Monitoring of Small Seismic/Acoustic Events," *Proceedings of the 18th Annual Seismic Research Symposium on Monitoring a Comprehensive Test Ban Treaty*, edited by J.F. Lewkowicz, J.M. McPhetres and D.T. Reiter, Annapolis MD, PL-TR-96-2153, ADA313692.

Konya and Walter (1990), *Surface Blast Design*, Prentice Hall, 303 pages.

McLaughlin, K.L., T.G. Barker and J.L. Stevens (1994), "Numerical Simulation of Quarry Blast Sources," S-CUBED Final Report to Phillips Laboratory, Kirtland AFB, SSS-TR-94-14418. ADA275799

McLaughlin, K. L., J. Bonner and T. G. Barker (1996), "Seismic Source Mechanisms for Quarry Blasts Observed Rayleigh and Love Wave Radiation Patterns from a Texas Quarry," in preparation.

Stump, B.W. and R.E. Reinke (1988), "Experimental Confirmation of Superposition from Small-Scale Explosions," *Bull. Seism. Soc. Am.*, **78**, pp. 1059-1073

Stump, B.W., D.C. Pearson, R.L. Martin, P.E. Harben, C.L. Edwards, D. Baker, K. Kihara, K. Dalrymple, J.P. Lewis, D. Rock and R. Boyd, "The Black Thunder Regional Seismic Experiment," LANL Report LAUL-95-3980.

Taylor, S.R. and G.E. Randall (1989), "The Effects of Spall on Regional Seismograms," *Geophys. Res. Lett.*, **16**, 211-214.

THOMAS AHRENS
SEISMOLOGICAL LABORATORY 252-21
CALIFORNIA INST. OF TECHNOLOGY
PASADENA, CA 91125

AIR FORCE RESEARCH LABORATORY
ATTN: RESEARCH LIBRARY/TL
5 WRIGHT STREET
HANSCOM AFB, MA 01731-3004

RALPH ALEWINE
NTPO
1901 N. MOORE STREET, SUITE 609
ARLINGTON, VA 22209

T.G. BARKER
MAXWELL TECHNOLOGIES
8888 BALBOA AVE.
SAN DIEGO, CA 92123-1506

THERON J. BENNETT
MAXWELL TECHNOLOGIES
11800 SUNRISE VALLEY
SUITE 1212
RESTON, VA 22091

JONATHAN BERGER
UNIV. OF CALIFORNIA, SAN DIEGO
SCRIPPS INST. OF OCEANOGRAPHY IGPP, 0225
9500 GILMAN DRIVE
LA JOLLA, CA 92093-0225

LESLIE A. CASEY
DEPT. OF ENERGY/NN-20
1000 INDEPENDENCE AVE. SW
WASHINGTON DC 20585-0420

ANTON DAINTY
HQ DSWA/PMA
6801 TELEGRAPH ROAD
ALEXANDRIA, VA 22310-3398

DIANE DOSER
DEPT. OF GEOLOGICAL SCIENCES
THE UNIVERSITY OF TEXAS AT EL PASO
EL PASO, TX 79968

MARK D. FISK
MISSION RESEARCH CORPORATION
735 STATE STREET
P.O. DRAWER 719
SANTA BARBARA, CA 93102-0719

AIR FORCE RESEARCH LABORATORY
ATTN: VSOE
29 RANDOLPH ROAD
HANSCOM AFB, MA 01731-3010   (2 COPIES)

AIR FORCE RESEARCH LABORATORY
ATTN: AFRL/SUL
3550 ABERDEEN AVE SE
KIRTLAND AFB, NM 87117-5776 (2 COPIES)

MUAWIA BARAZANGI
INSTOC
3126 SNEE HALL
CORNELL UNIVERSITY
ITHACA, NY 14853

DOUGLAS BAUMGARDT
ENSCO INC.
5400 PORT ROYAL ROAD
SPRINGFIELD, VA 22151

WILLIAM BENSON
NAS/COS
ROOM HA372
2001 WISCONSIN AVE. NW
WASHINGTON DC 20007

ROBERT BLANDFORD
AFTAC
1300 N. 17TH STREET
SUITE 1450
ARLINGTON, VA 22209-2308

CENTER FOR MONITORING RESEARCH
ATTN: LIBRARIAN
1300 N. 17th STREET, SUITE 1450
ARLINGTON, VA 22209

CATHERINE DE GROOT-HEDLIN
UNIV. OF CALIFORNIA, SAN DIEGO
IGPP
8604 LA JOLLA SHORES DRIVE
SAN DIEGO, CA 92093

DTIC
8725 JOHN J. KINGMAN ROAD
FT BELVOIR, VA 22060-6218 (2 COPIES)

LORI GRANT
MULTIMAX, INC.
311C FOREST AVE. SUITE 3
PACIFIC GROVE, CA 93950

HENRY GRAY
SMU STATISTICS DEPARTMENT
P.O. BOX 750302
DALLAS, TX 75275-0302

I. N. GUPTA
MULTIMAX, INC.
1441 MCCORMICK DRIVE
LARGO, MD 20774

DAVID HARKRIDER
BOSTON COLLEGE
INSTITUTE FOR SPACE RESEARCH
140 COMMONWEALTH AVENUE
CHESTNUT HILL, MA 02167

THOMAS HEARN
NEW MEXICO STATE UNIVERSITY
DEPARTMENT OF PHYSICS
LAS CRUCES, NM 88003

MICHAEL HEDLIN
UNIVERSITY OF CALIFORNIA, SAN DIEGO
SCRIPPS INST. OF OCEANOGRAPHY
9500 GILMAN DRIVE
LA JOLLA, CA 92093-0225

DONALD HELMBERGER
CALIFORNIA INST. OF TECHNOLOGY
DIV. OF GEOL. & PLANETARY SCIENCES
SEISMOLOGICAL LABORATORY
PASADENA, CA 91125

EUGENE HERRIN
SOUTHERN METHODIST UNIVERSITY
DEPT. OF GEOLOGICAL SCIENCES
DALLAS, TX 75275-0395

ROBERT HERRMANN
ST. LOUIS UNIVERSITY
DEPT. OF EARTH & ATMOS. SCIENCES
3507 LACLEDE AVENUE
ST. LOUIS, MO 63103

VINDELL HSU
HQ/AFTAC/TTR
1030 S. HIGHWAY A1A
PATRICK AFB, FL 32925-3002

RONG-SONG JIH
HQ DSWA/PMA
6801 TELEGRAPH ROAD
ALEXANDRIA, VA 22310-3398

THOMAS JORDAN
MASS. INST. OF TECHNOLOGY
BLDG 54-918
CAMBRIDGE, MA 02139

LAWRENCE LIVERMORE NAT'L LAB
ATTN: TECHNICAL STAFF (PLS ROUTE)
PO BOX 808, MS L-175
LIVERMORE, CA 94551

LAWRENCE LIVERMORE NAT'L LAB
ATTN: TECHNICAL STAFF (PLS ROUTE)
PO BOX 808, MS L-208
LIVERMORE, CA 94551

LAWRENCE LIVERMORE NAT'L LAB
ATTN: TECHNICAL STAFF (PLS ROUTE)
PO BOX 808, MS L-202
LIVERMORE, CA 94551

LAWRENCE LIVERMORE NAT'L LAB
ATTN: TECHNICAL STAFF (PLS ROUTE)
PO BOX 808, MS L-205
LIVERMORE, CA 94551

LAWRENCE LIVERMORE NAT'L LAB
ATTN: TECHNICAL STAFF (PLS ROUTE)
PO BOX 808, MS L-200
LIVERMORE, CA 94551

LAWRENCE LIVERMORE NAT'L LAB
ATTN: TECHNICAL STAFF (PLS ROUTE)
PO BOX 808, MS L-221
LIVERMORE, CA 94551

THORNE LAY
UNIV. OF CALIFORNIA, SANTA CRUZ
EARTH SCIENCES DEPARTMENT
EARTH & MARINE SCIENCE BUILDING
SANTA CRUZ, CA 95064

ANATOLI L. LEVSHIN
DEPARTMENT OF PHYSICS
UNIVERSITY OF COLORADO
CAMPUS BOX 390
BOULDER, CO 80309-0309

JAMES LEWKOWICZ
WESTON GEOPHYSICAL CORP.
325 WEST MAIN STREET
NORTHBORO, MA 01532

LOS ALAMOS NATIONAL LABORATORY
ATTN: TECHNICAL STAFF (PLS ROUTE)
PO BOX 1663, MS F659
LOS ALAMOS, NM 87545

LOS ALAMOS NATIONAL LABORATORY
ATTN: TECHNICAL STAFF (PLS ROUTE)
PO BOX 1663, MS F665
LOS ALAMOS, NM 87545

LOS ALAMOS NATIONAL LABORATORY
ATTN: TECHNICAL STAFF (PLS ROUTE)
PO BOX 1663, MS C335
LOS ALAMOS, NM 87545

GARY MCCARTOR
SOUTHERN METHODIST UNIVERSITY
DEPARTMENT OF PHYSICS
DALLAS, TX 75275-0395

KEITH MCLAUGHLIN
CENTER FOR MONITORING RESEARCH
SAIC
1300 N. 17TH STREET, SUITE 1450
ARLINGTON, VA 22209

BRIAN MITCHELL
DEPARTMENT OF EARTH & ATMOSPHERIC SCIENCES
ST. LOUIS UNIVERSITY
3507 LACLEDE AVENUE
ST. LOUIS, MO 63103

RICHARD MORROW
USACDA/IVI
320 21ST STREET, N.W.
WASHINGTON DC 20451

JOHN MURPHY
MAXWELL TECHNOLOGIES
11800 SUNRISE VALLEY DRIVE
SUITE 1212
RESTON, VA 22091

JAMES NI
NEW MEXICO STATE UNIVERSITY
DEPARTMENT OF PHYSICS
LAS CRUCES, NM 88003

ROBERT NORTH
CENTER FOR MONITORING RESEARCH
1300 N. 17th STREET, SUITE 1450
ARLINGTON, VA 22209

OFFICE OF THE SECRETARY OF DEFENSE
DDR&E
WASHINGTON DC 20330

JOHN ORCUTT
INST. OF GEOPH. & PLANETARY PHYSICS
UNIV. OF CALIFORNIA, SAN DIEGO
LA JOLLA, CA 92093

PACIFIC NORTHWEST NAT'L LAB
ATTN: TECHNICAL STAFF (PLS ROUTE)
PO BOX 999, MS K6-48
RICHLAND, WA 99352

PACIFIC NORTHWEST NAT'L LAB
ATTN: TECHNICAL STAFF (PLS ROUTE)
PO BOX 999, MS K6-40
RICHLAND, WA 99352

PACIFIC NORTHWEST NAT'L LAB
ATTN: TECHNICAL STAFF (PLS ROUTE)
PO BOX 999, MS K6-84
RICHLAND, WA 99352

PACIFIC NORTHWEST NAT'L LAB
ATTN: TECHNICAL STAFF (PLS ROUTE)
PO BOX 999, MS K5-12
RICHLAND, WA 99352

FRANK PILOTTE
HQ AFTAC/TT
1030 S. HIGHWAY A1A
PATRICK AFB, FL 32925-3002

KEITH PRIESTLEY
DEPARTMENT OF EARTH SCIENCES
UNIVERSITY OF CAMBRIDGE
MADINGLEY RISE, MADINGLEY ROAD
CAMBRIDGE, CB3 OEZ UK

JAY PULLI
BBN SYSTEMS AND TECHNOLOGIES, INC.
1300 NORTH 17TH STREET
ROSSLYN, VA 22209

DELAINE REITER
AFRL/VSOE (SENCOM)
73 STANDISH ROAD
WATERTOWN, MA 02172

MICHAEL RITZWOLLER
DEPARTMENT OF PHYSICS
UNIVERSITY OF COLORADO
CAMPUS BOX 390
BOULDER, CO 80309-0309

CHANDAN SAIKIA
WOOODWARD-CLYDE FED. SERVICES
566 EL DORADO ST., SUITE 100
PASADENA, CA 91101-2560

SANDIA NATIONAL LABORATORY
ATTN: TECHNICAL STAFF (PLS ROUTE)
DEPT. 9311
MS 1159, PO BOX 5800
ALBUQUERQUE, NM 87185-1159

SANDIA NATIONAL LABORATORY
ATTN: TECHNICAL STAFF (PLS ROUTE)
DEPT. 5736
MS 0655, PO BOX 5800
ALBUQUERQUE, NM 87185-0655

AVI SHAPIRA
SEISMOLOGY DIVISION
IPRG
P.O.B. 2286 NOLON 58122 ISRAEL

MATTHEW SIBOL
ENSCO, INC.
445 PINEDA CT.
MELBOURNE, FL 32940

JEFFRY STEVENS
MAXWELL TECHNOLOGIES
8888 BALBOA AVE.
SAN DIEGO, CA 92123-1506

TACTEC
BATTELLE MEMORIAL INSTITUTE
505 KING AVENUE
COLUMBUS, OH 43201 (FINAL REPORT)

LAWRENCE TURNBULL
ACIS
DCI/ACIS
WASHINGTON DC 20505

PAUL RICHARDS
COLUMBIA UNIVERSITY
LAMONT-DOHERTY EARTH OBSERV.
PALISADES, NY 10964

DAVID RUSSELL
HQ AFTAC/TTR
1030 SOUTH HIGHWAY A1A
PATRICK AFB, FL 32925-3002

SANDIA NATIONAL LABORATORY
ATTN: TECHNICAL STAFF (PLS ROUTE)
DEPT. 5704
MS 0979, PO BOX 5800
ALBUQUERQUE, NM 87185-0979

SANDIA NATIONAL LABORATORY
ATTN: TECHNICAL STAFF (PLS ROUTE)
DEPT. 5704
MS 0655, PO BOX 5800
ALBUQUERQUE, NM 87185-0655

THOMAS SERENO JR.
SAIC
10260 CAMPUS POINT DRIVE
SAN DIEGO, CA 92121

ROBERT SHUMWAY
410 MRAK HALL
DIVISION OF STATISTICS
UNIVERSITY OF CALIFORNIA
DAVIS, CA 95616-8671

DAVID SIMPSON
IRIS
1200 NEW YORK AVE., NW
SUITE 800
WASHINGTON DC 20005

BRIAN SULLIVAN
BOSTON COLLEGE
INSITUTE FOR SPACE RESEARCH
140 COMMONWEALTH AVENUE
CHESTNUT HILL, MA 02167

NAFI TOKSOZ
EARTH RESOURCES LABORATORY
M.I.T.
42 CARLTON STREET, E34-440
CAMBRIDGE, MA 02142

GREG VAN DER VINK
IRIS
1200 NEW YORK AVE., NW
SUITE 800
WASHINGTON DC 20005

FRANK VERNON
UNIV. OF CALIFORNIA, SAN DIEGO
SCRIPPS INST. OF OCEANOGRAPHY
9500 GILMAN DRIVE
LA JOLLA, CA 92093-0225

JILL WARREN
LOS ALAMOS NATIONAL LABORATORY
GROUP NIS-8
P.O. BOX 1663
LOS ALAMOS, NM 87545   (5 COPIES)

RU SHAN WU
UNIV. OF CALIFORNIA, SANTA CRUZ
EARTH SCIENCES DEPT.
1156 HIGH STREET
SANTA CRUZ, CA 95064

JAMES E. ZOLLWEG
BOISE STATE UNIVERSITY
GEOSCIENCES DEPT.
1910 UNIVERSITY DRIVE
BOISE, ID 83725

TERRY WALLACE
UNIVERSITY OF ARIZONA
DEPARTMENT OF GEOSCIENCES
BUILDING #77
TUCSON, AZ 85721

DANIEL WEILL
NSF
EAR-785
4201 WILSON BLVD., ROOM 785
ARLINGTON, VA 22230

JIAKANG XIE
COLUMBIA UNIVERSITY
LAMONT DOHERTY EARTH OBSERV.
ROUTE 9W
PALISADES, NY 10964